

Published in final edited form as:

J Mater Chem B Mater Biol Med. 2014 May 28; 2(20): 2958–2973. doi:10.1039/C4TB00094C.

Rare Earth Nanoprobes for Functional Biomolecular Imaging and Theranostics

Dominik J. Naczynski^{1,4}, Mei Chee Tan^{2,3}, Richard E. Riman³, and Prabhas V. Moghe^{4,*}

¹Department of Radiation Oncology, Stanford University School of Medicine, California, USA

²Engineering Product Development, Singapore University of Technology and Design, Singapore

³Department of Materials Science and Engineering, Rutgers University, New Jersey, USA

⁴Department of Biomedical Engineering, Department of Chemical & Biochemical Engineering, Rutgers University, New Jersey, USA

Abstract

Contrast agents designed to visualize the molecular mechanisms underlying cancer pathogenesis and progression have deepened our understanding of disease complexity and accelerated the development of enhanced drug strategies targeted to specific biochemical pathways. For the next generation probes and imaging systems to be viable, they must exhibit enhanced sensitivity and robust quantitation of morphologic and contrast features, while offering the ability to resolve the disease-specific molecular signatures that may be critical to reconstitute a more comprehensive portrait of pathobiology. This feature article provides an overview on the design and advancements of emerging biomedical optical probes in general and evaluates the promise of rare earth nanoprobes, in particular, for molecular imaging and theranostics. Combined with new breakthroughs in nanoscale probe configurations, and improved dopant compositions, and multimodal infrared optical imaging, rare-earth nanoprobes can be used to address a wide variety of biomedical challenges, including deep tissue imaging, real-time drug delivery tracking and multispectral molecular profiling.

1. Introduction

The growing interest in molecular imaging has initiated new research efforts in the field of materials chemistry geared toward improved probe designs, more sensitive imaging platforms and localized reporting of disease-specific molecular biology. Molecular imaging (MI) aims to identify and track molecular and cellular pathogenesis within the natural environment of live tissues and organs. These events can cover a wide spectrum of cases including the location, identification and characterization of diseased lesions defined by a specific class or type of molecular targets, or the quantification of protein receptor expression levels on the surface of cells which may be potentially used as an indicator of disease progression. In contrast to conventional method of studying these events *in vitro* or *ex vivo*, MI aims to elucidate the molecular phenotypes of tissues where the cells and tissues

*To whom correspondence should be addressed. Prabhas V. Moghe, Distinguished Professor, Department of Biomedical Engineering, Rutgers University, 599 Taylor Road, Piscataway, NJ 08854, moghe@rutgers.edu.

are evolving in dynamic reciprocity with their microenvironment and where the related feedback loop for the molecular pathways remain intact. The ability to monitor molecular and cellular events in a living animal or human has major implications for monitoring drug mechanisms during pre-clinical drug discovery and validation, and can guide significant improvements in disease management and the dissection of the key links between pharmacobiology and pathobiology.

The identification of the molecular targets mediating disease pathogenesis and progression has resulted in more accurate disease prognoses and a wider range of clinical treatment strategies, ushering in an age of personalized patient care and molecularly targeted therapies. Technologies for imaging molecular cues and events in patients are becoming increasingly critical when monitoring the complex behavior demonstrated by many diseases such as cancer.^{1, 2} In particular, optical imaging has emerged as a noninvasive molecular imaging modality that is inherently safe,³⁻⁶ offers high sensitivity,^{7, 8} and requires relatively inexpensive and portable instruments that enable rapid clinical integration.⁸ However, resolving at the molecular scale requires the development of probes that can selectively target specific biological features and enhance image contrast. Imaging probes have therefore become important tools for improving the contrast-to-background ratios (CNR) to allow one to “see” and clearly identify the molecular targets of interest for MI applications.

This feature article will provide an overview on the design and advances of new generation biomedical optical probes and highlight emerging clinical areas of impact that can be envisioned in the near future. A typical imaging probe will comprise of: (1) chemically specific functional group(s) that interacts with intended molecular target, (2) a signaling component which produces the signal contrast and (3) a linker that chemically bonds these first two components together. If the imaging probe can be constructed to include a therapeutic component, then the resulting probe which serves as both a contrast agent and therapeutic will enable “theranostics”. The chemical development of multimodal probes that support complementary imaging on multiple imaging platforms will also be discussed briefly in this paper.

2. Emerging Frontiers of Optical Molecular Imaging in Nanomedicine

Nanoparticle probes are promising candidates for optical detection and offer distinct advantages when compared to other classes of contrast agents, such as organic fluorophores. Composed of one or more inorganic and/or organic materials, nanoparticles are colloidal systems (1–100 nm) that offer a highly versatile material platform, which can be rationally engineered to address specific design requirements, such as favorable biocompatibility, multivalent biomarker targeting and controlled pharmacokinetic behavior.⁹⁻¹³ By modifying parameters such as size, surface charge and shape, nanoparticles can be tailored for prolonged circulation and reduced clearance *in vivo*.¹⁴⁻¹⁷ In addition to physical modifications, the surfaces of nanoparticles can be decorated with amphiphilic coatings, such as polyethylene glycol (PEG) polymers, or targeting ligands and antibodies.¹⁸ These chemical modifications can lead to enhancements in biocompatibility, reductions in nonspecific biological interactions, and improvements in molecular targeting specificity.¹⁸

Critically, nanoparticle optical imaging agents must be detectable by light in biological tissues to have translatable utility for *in vivo* molecular imaging. As light travels through increasing depths of tissue, photons are either absorbed or scattered.¹⁹ The result of absorption is attenuation in the intensity of the propagating light as well as the occurrence of tissue-induced autofluorescence.⁹ Near infrared light (NIR, 700–1000 nm) is absorbed less by tissue components than visible light,²⁰ resulting in greater penetration and thus, deeper detection of imaging probes²¹ in the first “tissue transparent window.” Light scattering caused by cellular components in tissue is another major cause of signal attenuation and dominates over absorption in certain regions of the spectrum (See Fig. 1a).^{22–24} Scattering changes the original direction of propagating light and obscures the spatial position of probes in tissue. Although scattering is strongly dependent on tissue composition, longer wavelengths in the shortwave infrared (SWIR, 1000–2300 nm) can lead to significant reductions in scattering when compared to the NIR (See Fig. 1b).

Optimal nanoparticle-based optical imaging probes are those designed to detect infrared emissions and improve the CNR for a targeted molecular feature, produce intense emission signals after excitation, resist quenching or photobleaching, offer tunable optical characteristics and exhibit biological and chemical stability. Although NIR-detectable nanomaterial agents such as quantum dots (QDs) and single-walled carbon nanotubes (SWNTs) have been extensively investigated for biomedical imaging applications and reviewed elsewhere,^{25–27} recent work with **rare-earth-doped nanoprobles (REs)** has provided evidence that this class of nanoparticles has enormous potential and significant advantages over other agents for optical molecular imaging.²⁸ Therefore, this review is focused on the design, synthesis, properties and applications of RE nanoprobles as a promising class of biophotonic materials.

3. Rare Earth Nanoprobles

3.1 General properties and synthesis

REs are inorganic crystalline nanostructures composed of a host material (such as NaYF₄) that has been doped with one or more rare-earth dopants. They are generally fabricated as core-shell particles with the nanoparticle core comprised of the host material and dopants, while the undoped host material shell envelops the inner doped structure. In addition to protecting the dopants from degradation, the shell acts to both minimize surface quenching effects and improve optical efficiency.²⁹ Due to the numerous energy level transitions offered by the fourteen rare-earth elements, REs offer a wide range of emission profiles that are tailored by selecting the appropriate dopant(s). (See Fig. 2).^{30–37}

REs are generally fabricated through a solvothermal synthesis method. Solvothermal synthesis is a solution chemistry approach that provides a uniform chemical environment to crystallize anhydrous ceramic materials of different sizes and morphologies directly from solution. In a typical reaction, solutions, suspensions, or gels are prepared from soluble and insoluble compounds that are subsequently reacted in a solvent (water or an organic solvent) at carefully chosen temperature and pressure.^{37–48} For example, oxides, nitrates, chlorides, acids and bases can be dissolved in a reaction medium that can be either aqueous, non-aqueous (e.g., polyol, oleic acid, ethanol or octadecene) solvents or a mixture of any above-

mentioned fluids. The solvothermal synthesis method has been used to grow various rare-earth doped particles with controlled micron- to nano-sizes and morphologies by adjusting the reaction parameters, like precursor concentration, time and solvent.^{29, 37, 39, 41, 42, 45, 47, 49–52} For example, the thermal decomposition of rare earth trifluoroacetate precursors in solvents such as oleic acid or oleylamine under temperatures 250–350°C is commonly used to synthesize crystalline monodisperse REs of tailored size.^{42, 53, 45}

A systematic study on the effects of particle size on the upconversion and down-shifting optical properties was conducted using a series of monodisperse β -NaYF₄:Yb,Er nanocrystals with sizes ranging from 11 to 110 nm which were synthesized using a solvothermal decomposition method (see Fig. 3).⁴² It was observed that the intensities of the upconversion and down-shifting emissions spanning the visible to IR regions were reduced as particle size decreased. The time-resolved transient spectrometry measure of the $^4I_{13/2} \rightarrow ^4I_{15/2}$ transition revealed a reduction of the internal quantum efficiency from 50 to 15%, for particle sizes of 110 and 11 nm, respectively. The reduction in internal quantum efficiency with decreasing particle sizes was attributed to the surface –OH quenching effects which dominated the overall non-radiative relaxation mechanism. The contribution of multiphonon relaxation to the overall non-radiative mechanism decreased while the influence of surface –OH quenching increased with decreasing particle size. Surface –OH quenching rates were calculated to be ~4 times higher than that of the multiphonon relaxation rates, and thus, primarily controls emission intensity for these materials.

3.2 Tunable Optical Properties of REs

REs can be excited with NIR to emit in both the visible and infrared region of the electromagnetic spectrum, through the upconversion and down-shifting process, respectively (see Fig. 4).^{54,55} Upconversion fluorescence occurs during the excitation of trivalent rare earth ions by the sequential absorption of two or more NIR photons, which results in the nanoparticles reaching a higher excited energy level.^{53, 56, 57} The upconversion fluorescence process can occur through three main mechanisms: excited state absorption (ESA), photon avalanche and energy transfer upconversion (ETU). Of these three, co-doped NaYF₄ nanoparticles rely primarily on ETU for upconversion,⁵⁸ and the ETU mechanism is considered to be the most efficient upconversion process known.⁵⁹ For NaYF₄ co-doped REs, upconversion fluorescence occurs following the non-radiative transfer of excitation energy from a sensitizer, such as Yb, to an activator such as Er or Tm, resulting in the emission of photons with a different energy.⁵⁹

For energy transfer to occur, the excited energy levels of both the sensitizer and activator must be nearly equal (or resonant) and the two ions must be in close spatial proximity with one another. Trivalent Yb resonates with several upconverting lanthanide ions, such as Er, Tm, Ho, Pr, Gd, Nd, and Dy,⁶⁰ acting as a very efficient sensitizer for energy transfer.⁵⁸ In general, the emitted light intensity increases with the increasing concentration of the emitting ion. However, the emission intensity is observed to increase up to a critical concentration of emitting ions. At this concentration the emission intensity decreases due to

one or more energy transfer mechanisms (e.g., cross relaxation) between emitting ions, through a process known as concentration quenching.

REs can also emit SWIR after NIR excitation through down-shifting fluorescence mechanisms.^{38, 41, 61–64} Examples of SWIR-emitting down-shifting materials can be seen with Nd-doped yttrium aluminum garnet (Nd:YAG),⁶⁵ a solid state laser material that emits at 1064 nm after 800 nm excitation, and Er-doped silicate glass fibers,⁶⁶ which are commonly used for telecommunications using the 1550 nm emission via 980 nm excitation.⁵⁵ Theoretical calculations founded on first principles enabled the design and selection of unique dopant chemistries that result in bright emissions at the tailored wavelengths. First principle calculations have elucidated the contributing factors of the local atomic environment, such as crystal field strength, site symmetry, electron-phonon interaction strength of the dopants, which controls the absorption and emission behavior of rare-earth doped phosphors. In addition, the multiphonon relaxation rates and concentration quenching mechanisms governs the efficiency of the allowable transitions.

The choice of host material determines the emission efficiency for a given transition. Numerous hosts, such as oxides (e.g., silicate, yttrium oxide), halides, tellurites, borates, germanates, phosphates and vanadates have been evaluated and reported in the literature for their potential as brightly-emitting rare earth doped hosts.^{26, 33, 35, 36, 55, 62, 65–68} However, since the number of phonons required to bridge the energy gap of the desired transition is higher in low phonon energy hosts, the likelihood for non-radiative losses are lesser and radiative transitions are more likely to occur. Therefore, low phonon energy halide hosts (e.g., NaYF₄, LaF₃, YF₃, CaF₂) that enable bright emissions through minimization of non-radiative losses are favored. NaYF₄ have been shown to display low phonon energies, high chemical stability and high optical transparency ideal for upconversion processes.⁵⁸ In addition, the crystalline structure of the host can influence the efficiency of upconversion. For example, hexagonal phase NaYF₄ has been shown to exhibit significantly greater upconversion efficiencies compared to cubic phase NaYF₄.^{39, 53, 69} In addition, the host material may also interact and enhance energy transfer to the rare-earth luminescent center in a manner that facilitates the desired emission while avoiding secondary emissions that are not of interest. For example, we have reported that when Yb, Er were doped in CeF₃, only the infrared emission at 1530 nm was observed while all of the typical visible upconversion emissions were absent.⁶⁴ The increase in infrared emission intensity is achieved by changing the branching ratio for the 1530 nm emission from 0.1–0.2 to 0.8–0.9. Further studies to develop a deeper understanding on the effects of host interactions on the branching ratios are warranted. In addition, whilst the low phonon energies of the halide hosts facilitate brighter emissions, especially in the infrared region, a common trade-off is the poor physical and chemical stability of halides. Therefore, investigations on alternative hosts or chemical modifications to enhance the host stability will open new avenues in the development of next generation infrared-emitting probes.

Surface modifying agents can also strongly affect the optical properties of REs. For example, the hydrocarbon (-CH₂) and hydroxyl (-OH) groups present on surfactants used during synthesis can deactivate surface rare-earth ions on REs and result in emission quenching.⁴¹ We have previously investigated the effects various surfactant formulations

have on RE emission using micron-sized particles. NaYF₄:Yb-Er were synthesized using the hydrothermal method and subsequently modified with low concentrations of different surfactants. We found that trioctylphosphine, PEG monooleate and polyvinylpyrrolidone (PVP) exhibited significantly different optical efficiencies (see Fig. 6).⁷⁰ The emissions of PVP-modified REs were found to be significantly brighter than the unmodified particles with a higher optical efficiency. The improvement in optical efficiency was attributed to reduced reflectance losses that occur at the particle-air interface via mismatching of refractive indexes. Prior to this study, surfactant selection was guided primarily on how coating will affect particle morphology and dispersion properties, ignoring the effects refractive index mismatch will have on RE optical properties. This work highlights the importance in surfactant selection for designing highly emissive REs.

4. Biomedical applications

4.1 REs for biomedical applications

REs have been widely investigated for various biomedical applications due to their advantageous optical characteristics, such as narrow emission bandwidths, large Stokes shifts, long fluorescence lifetimes and photostability, relatively biocompatible compositions and tunable physical properties.^{58, 71–74} In addition, by controlling synthesis chemistry, a wide range of emissions can be generated by REs for multispectral imaging, which can be used to develop a library of probes for simultaneously imaging multiple molecular processes in biological tissue.

Effective RE imaging formulations must consider the way in which probe features impact biological functionality. For example, physical characteristics such as size, surface charge and shape play important roles in dictating the biodistribution and clearance of nanoparticles in circulation. Probe biocompatibility and stability in circulation are also critical parameters often overlooked when new formulations are designed. REs must exhibit a favorable safety profile in order to have any real potential towards clinical translation. Otherwise, the use of any new formulations will be largely limited to *in vitro* and small animal pre-clinical testing.

4.2 RE Probe Size

Probe size is an important physical property that has been shown to greatly affect nanoparticle behavior in circulation.^{12, 13} The lower boundary of nanoparticle size is generally considered to be around 10 nm in diameter, the estimated threshold for first-pass elimination by the kidneys. The upper boundary, however, is less defined and not entirely clear. Particles must be sufficiently small to avoid unwanted accumulation in the lungs or filtration by the liver, yet still be capable of eventually being cleared.

In cancer, many tumor vessels tend to exhibit irregular branching patterns and abnormal architecture, a consequence of poorly-aligned endothelial cells with wide fenestrations and loose focal intercellular openings. These unique properties of the tumor microenvironment lead to a “leaky” endothelium, enabling larger macromolecules, such as nanoparticles, to accumulate in tumor tissue much more than in normal, healthy tissue.⁷⁵ Experiments have shown that the threshold for this so-called enhanced permeability and retention (EPR) effect may be approximately 400 nm but that sizes of carriers below 150 nm are more effective at

accumulating in the tumor tissue.^{76–79} Evidence has confirmed that this phenomenon occurs in humans as well as in animal models. Nanoparticle delivery that relies on the EPR effect is commonly referred to as “passive targeting” and can result in the selective extravasation of certain type of particles into solid tumors.

4.3 Surface properties of RE Nanoparticles

Like other nanoparticles, the surface properties of REs play a critical role in determining their biological properties.^{12, 13, 80, 81} *In vivo* experiments have shown that slightly negative, slightly positive or neutral nanoparticles can penetrate and be effectively transported through tissue.^{10, 82, 83} As-synthesized REs are generally hydrophobic and lack functional groups for the conjugation of molecular targeting agents. REs can be modified with coatings, such as polyethylene glycol (PEG) polymers, to improve hydrophilicity and reduce their self-aggregation tendency in aqueous solutions by creating a hydrated layer around each nanoparticle. PEG coatings, in particular, have been used to promote the biocompatibility and reduce nonspecific interactions of nanoparticles with biomolecules.^{18, 84} Other surface modifications including coating with silica,^{85, 86} mercaptopropionic acid,⁸⁷ diphosphonic acid,⁸⁸ and polymer surfactants such as polyethyleneimine (PEI)^{89–91} have been investigated to render REs hydrophilic. Although modifying REs with silica has been reported to increase emission intensity, it is difficult to coat the nanoparticles uniformly, and still requires additional modification chemistry in order to generate surface functional groups for bioconjugation.⁹¹ In addition, the toxicity of many surface coating reagents must be taken into consideration before exposing living systems to modified REs. For example, while there has been success with coating REs with PEI, its high charge density results in significant cytotoxicity.⁹²

Greater surface charges, whether positive or negative, increase the likelihood for nanoparticle opsonization, a process by which certain serum proteins adsorb onto the surface of nanoparticles and interact with monocytes or certain tissue macrophages. Opsonization leads to macrophage scavenging and greater clearance of nanoparticles by the reticuloendothelial system (RES), which consists of phagocytic cells in the liver, spleen and lymph nodes.¹⁰ While nanoparticle clearance is fundamentally important, minimizing rapid losses is crucial to realizing the utility of nanoparticles *in vivo*.

Although charge and steric stabilization provide improvements in systemic nanoparticle pharmacokinetics, non-uniform and untargeted biodistribution are additional limiting factors that prevent nanoparticles from effectively accumulating in diseased tissues.⁹³ This has led to the development of targeting ligands, which can be anchored to the surface of nanoparticles usually through covalent interactions. In contrast to passive delivery, targeting nanoparticles to specific molecular receptors using ligands is known as “active delivery”. The targeting ligands themselves can be chemical or biological moieties including compounds such as small molecules,⁹⁴ peptides,⁹⁵ or antibodies.⁹⁶ Such ligands improve or direct specific nanoparticle-cell interactions, enabling enhanced and modified accumulation at diseased tissue.

4.4 Biocompatibility of REs Nanoprobes

Ensuring the biocompatibility of any new RE formulation is essential for translating these agents *in vivo*. While numerous studies have reported on the minimal *in vitro* toxicity of REs within certain concentrations, there is limited information regarding the health effects of REs in larger animal models. Notably, Xiong et al. investigated the long term effects of polyacrylic acid-coated REs in athymic nude mice. They found mice injected with 15 mg/kg of REs showed no significant differences in organ histology, hematology and other biochemical indicators of toxicity compared to control mice after 115 days.⁹⁷ However, the group did observe slight abnormalities in the spleen, which was indicative of mild nanotoxicity.

Compared to many types of QDs comprised of lead, arsenic or cadmium, *REs are constituted of elements with better safety profiles*. In addition, the lanthanide species in REs are doped into the host at very low concentrations, with the majority of the probe being composed of a yttrium-based host. The LD50 values for intravenously injected yttrium and lanthanide salts has been determined to be between 10–100 mg/kg.⁹⁸ *Another relevant consideration is the toxicity of the formulated REs, and not merely that of the elemental REs. The processed RE probes* are structured, crystalline compounds that are much more stable and will likely exhibit more inert behavior in circulation.

Nevertheless, numerous groups have attempted to improve the biocompatibility of by modifying the surface with various molecules. For example, coating REs with PEG,^{84, 99} silica^{100, 101} and chitosan^{102, 103} has been shown to improve the biological tolerance of REs as well as their aqueous solubility and functionality for applications in disease targeting and drug delivery.

We have developed a novel approach for fabricating hydrophilic and biocompatible REs by encapsulation with human serum albumin, a common protein found in blood plasma with a history of FDA-approval (see Fig. 5).¹⁰⁴ Our approach is versatile and robust – it permits strict control of the albumin “shell” deposition to yield rare-earth-albumin nanocomposites ranging in size from 75–275 nm with narrow polydispersity and high, long-term stability in aqueous solutions. The nanocomposites exhibited significantly improved biocompatibility over non-encapsulated REs and offered surface amine groups that could be utilized for bioconjugating antibodies, peptides or other ligands for disease biomarker targeting. As proof-of-concept, we modified the nanocomposites with cyclic RGD to target glioblastoma cells expressing a well-known tumor biomarker, the $\alpha V\beta 3$ integrin receptor (see Fig. 5). We have also shown that encapsulation within albumin can modulate the biodistribution, improve the pharmacokinetics and magnify the tumor tissue accumulation of the REs *in vivo*.²⁸ Thus, our work offers a possible route for altering the biological behavior of other nanoparticle formulations, such as quantum dots, magnetic and gold nanoparticles. Finally, the ability of albumin to bind readily with a number of therapeutic drugs, coupled with its biodegradability and preferential uptake into tumor tissues, make it an ideal candidate for drug delivery purposes.¹⁰⁵

4.5 Upconversion Fluorescence of REs

One method of visualizing REs is through NIR-induced upconversion phosphorescence. Upconversion is an anti-Stokes process that involves the absorption of two or more low energy NIR photons (typically 980 nm) by REs followed by an emission of one higher energy photon in the visible range. Since this process does not naturally occur in living systems, imaging REs through upconversion results in very low nonspecific background fluorescence and consequently greatly improved CNR values.¹⁰⁶

In addition, the use of NIR offers other advantages for biomedical applications of REs.^{107, 108} Briefly, NIR is a non-ionizing form of radiation, minimizing tissue damage when used at reasonable power densities and durations.⁶ NIR light sources, such as laser diodes, are portable and inexpensive devices that are widely available and easily miniaturized that can be easily implemented into many pre-clinical and clinical settings. NIR-based imaging can also be performed in real-time, enabling molecular imaging to be performed rapidly and longitudinally.

The optical characteristics of tissue components support additional attributes that inherently favor NIR imaging. When visible or UV light interacts with tissue, absorption losses caused by chromophores such as water, hemoglobin, lipids and melanin limit the penetration depth of visible light to several millimeters.^{9, 109} In addition, there is also the possibility for nonspecific tissue autofluorescence to occur after light absorption. Tissue autofluorescence at these wavelengths can severely limit the signal-to-background ratio and decrease the sensitivity for exogenous agents such as nanoparticles. Chromophores such as elastin, collagen, tryptophan and porphyrins generally have absorption bands in the visible and UV regions of the spectrum and therefore can significantly contribute to autofluorescence and.¹¹⁰ NIR, on the other hand, exhibits relatively low tissue absorbance when compared to visible light, permitting deeper photon propagation in biological samples and reduced tissue autofluorescence.

4.6 Shortwave Infrared Emissions of REs

Visualizing REs through upconversion fluorescence is dependent on being able to detect visible light after NIR excitation. Although useful for *ex vivo*, *in vitro* and shallow, sub-surface *in vivo* imaging, visible light will be subjected to signal attenuation by surrounding chromophores in tissue. Furthermore, visible light can be subjected to scattering as it passes through tissue. Scattering is primarily the result of heterogeneities in the size, composition and morphology of cellular components in biological tissues.^{23, 24, 108, 111, 112} Scattering leads to the spreading, or defocusing, of optical signal and decreases imaging resolution. Longer wavelengths of light in regions such as the SWIR (1000–2300 nm) exhibit significantly decreased scattering in certain tissues. In fact, optical simulations have reported that SWIR can exhibit comparably low absorbance and tissue autofluorescence as NIR but up to a 1000-fold greater reduction in scatter losses.¹¹³ However, challenges exist for the widespread use of SWIR-based imaging. Few established standards are capable of efficiently generating SWIR while possessing the properties for safe translation into biomedical applications.¹¹⁴ Furthermore, there are no commercially available SWIR

imaging systems due to the need for special classes of cameras using indium gallium arsenide (InGaAs) semiconductor technology in order to detect SWIR light.

Currently available materials reported to exhibit SWIR emissions have numerous shortcomings including high toxicity, broad spectral emission and low quantum yield that must be overcome prior to clinical translation. For example, SWIR-emitting semiconducting quantum dots (QDs) made from materials such as HgTe, CdHgTe, InP, InAs, PbS, PbSe, and PbTe are comprised of several well-known toxic elements reducing their applicability in biomedical imaging.^{115, 116} Infrared-emitting single-walled carbon nanotubes (SWNTs) generate broad emissions of weak intensity and require high-powered, pulsed excitation sources which may result in localized tissue damage.^{117, 118}

Recent work has indicated that REs also exhibit SWIR emissions after NIR excitation.^{119, 120} In contrast to other SWIR-emitters, REs display narrow, intense emission peaks throughout the SWIR.^{28, 121} The optical efficiency of these RE-doped phosphors were compared with the conventional SWIR-emitting fluorophores such as organic dyes (IR-26), quantum dots (PbSe) and SWNTs (see Fig. 7).^{28, 121} The optical efficiency results show that the REs were excellent potential candidates as imaging probes since these significantly outperformed IR-26 and SWNT in brightness. They also show enhanced biocompatibility compared to quantum dots that are comprised of toxic Pb. We have recently reported on the first evidence of multi-spectral, real-time SWIR imaging offering anatomical resolution using REs and have demonstrated their applicability for identifying disease.²⁸ Our work has addressed the challenge of developing a biocompatible SWIR-emitting probe by fabricating REs with elements shown to have very low toxicity and clinical approval for implantation (e.g. yttrium).¹²² To this end, we have designed a low-cost imaging system capable of video-rate SWIR detection and rapid implementation within a preclinical or clinical setting. Compared to another similarly functioning system that has been reported in the literature,^{117, 118, 123} our prototype operates at significantly lower excitation power yet can achieve nanomolar detection sensitivity with 20-fold shorter exposure times to enable real-time imaging of rapid biological processes.

By changing the lanthanide dopant used in the RE core, discrete spectral emissions were produced across the SWIR region using a single NIR excitation source. Altogether, four distinguishable spectral patterns were produced using erbium, holmium, thulium and praseodymium dopant schemes. The ability to tune the SWIR emissions of REs opens the possibility for multispectral imaging and, with appropriate targeting approaches, molecular imaging using excitation and emission wavelengths that are both in a tissue transparent spectral region. The ability to image multiple sources of emission or contrast simultaneously in tissue has the potential to not only improve the reliability of the diagnoses but also provide insights into the complex interplay between various biological processes occurring in diseases such as cancer.^{124, 125}

4.7 Biomedical Applications of REs as Optical Probes

The unique physical and optical characteristics of REs have motivated efforts to investigate their use for numerous biomedical applications including molecular biosensing,^{126–130} image-guided drug pharmacokinetic screening,^{131–133} and anatomical and molecular disease

imaging.^{28, 57, 91, 97, 104, 134–136} In addition, REs have been studied as agent for photodynamic^{137–139} and photothermal^{140–142} therapies (PDT and PTT, respectively) as well as light-triggered^{143, 144} drug delivery applications. It is important to note that the use of any optical agent for biomedical applications faces inherent limitations due to the relatively shallow tissue penetration of light caused by absorption and scattering losses. This largely limits optical approaches to sub-surface (millimeter to centimeter) applications.

Phototherapy—PDT is a clinical strategy that in a typical embodiment utilizes cytotoxic singlet-state reactive oxygen species (ROS) generated by light for noninvasively treating diseases such as cancer. Typically, PDT consists of three components: photosensitizers (PS), light source and ROS present near targeted tissue. Excitation of photosensitizers at appropriate wavelengths results in the generation of ROS, which is cytotoxic to cells. Unfortunately, most PS can only be excited with low tissue penetrating UV or visible light, limiting their clinical applicability to disease sites readily accessible by light sources and present no more than a few millimeters below tissue surface. The upconversion fluorescence of REs has been proposed to be an effective means of triggering PS to generate ROS. NIR excitation of REs conjugated with PS can potentially find use for deeper tissue PDT of disease.

PTT is another type of cancer therapy in which agents in close proximity to diseased tissue are used to convert infrared light into heat. REs have been combined with elements such as gold and silver that have been shown to exhibit strong plasmonic resonance with NIR in order to induce PTT. Molecularly targeted REs bound with PTT-active agents can be used as a multifunctional agent that enables tumor tissue imaging, pharmacokinetic tracking, and therapeutic action all using the NIR excitation of REs.

Multimodal imaging—Numerous groups have investigated the use of REs as multimodal imaging agents. Multimodal imaging utilizes multiple imaging modalities to co-register visual information on several spatial scales simultaneously. Co-registering anatomical and molecular information can provide both the spatial localization and structure of diseases such as cancer as well as functional, metabolic and cellular characteristics.^{145, 146} For example, multimodality can be used as part of an imaging workflow, allowing clinicians to preoperatively identify cancer sites in patients and subsequently offer surgeons approaches to delineate the exact cellular margins of disease for surgical intervention through intraoperative imaging.^{146–149} Multimodal imaging functionalities using REs have been developed to combine upconversion fluorescence imaging (optical) with X-ray computed tomography (CT),^{150, 151} magnetic resonance imaging (MRI),^{87, 152–154} or positron emission tomography (PET).^{155, 156} Ultimately, modifying REs for multimodal imaging must take into consideration the benefits that will be achieved with a more complex imaging system as well as the impact of how modifications may alter the optical properties of REs.

Separately, a potentially exciting opportunity for multimodal imaging with REs that has not yet been investigated could lie with a novel imaging modality known as photoacoustic imaging. Photoacoustic imaging is a hybrid modality that uses an optical pulse to generate an acoustic signal which can be registered by ultrasound devices. Photoacoustic imaging relies on the excitation of a contrast agent with a pulse of laser light. Once excited, the

contrast agents produce very low amounts of heat which in turn generate a thermoelastic expansion resulting in a measurable ultrasound wave.¹⁵⁷ This technique combines both the sensitivity of optical imaging with the high spatial resolution provided by acoustic techniques such as ultrasound. This technique could be used to create 3-D maps of vasculature or determine the spatial position of the REs within an imaging-accessible tumor with NIR excitation and without changing existing formulation schemes.

SWIR Multiplex Imaging—To date, imaging with REs has been focused primarily on exploiting upconversion fluorescence after excitation with NIR light.¹⁰⁴ Recently, imaging using SWIR has gained attention as a means to improve signal detection depth and resolution for biomedical applications. Although this form of imaging is relatively new, researchers have reported on the use of REs for anatomical imaging of organs such as the liver using SWIR.^{67, 68} Our group has presented the first report on the use of REs for SWIR imaging of diseased tissue in the form of metastatic tumor lesions.²⁸ We chose to investigate targeting potential of REs following albumin encapsulation in a transgenic animal model that spontaneously develops dark, pigmented melanoma lesions shortly after birth (see Fig. 8). Notably, the SWIR emission signal was clearly observed even through dense, pigmented tumor tissue. We further explored the potential of REs as SWIR contrast agents for several important biomedical imaging applications including: 1) real-time probe detection, 2) tumor vascular imaging, and 3) multi-spectral signal resolution.

Following intravenous injection into mice, REs were observed throughout the vasculature network and tracked through individual organs such as the lungs and heart before accumulating in the liver and spleen (see Fig. 9). Transient SWIR emissions were observed in both the lungs and heart, confirming the circulation and whole-body distribution of the nanoparticles. Notably, video imaging clearly revealed pulsing SWIR emissions in the animal's chest, likely due to the movement of REs through the beating heart and lungs, providing evidence for the use of deeper-tissue SWIR imaging to rapidly evaluate nanoparticle biodistribution in real-time. Notably, in all locations where SWIR emission was observed in the mice, the upconversion fluorescence signal of the REs was absent, likely due to absorption and scattering losses caused by blood and tissue components.

To highlight the enhanced blood transmission of SWIR, tumor-burdened mice were injected with REs and imaged in real-time. Aberrant vascular patterns were observed near tumor xenografts during whole body imaging, which corresponded to tumor vasculature during intraoperative imaging (see Fig. 10). Both the feeder vessel and individual angiogenic blood vessels lining the tumor were easily resolved without any further modifications to the imaging system, in contrast to the earlier reports of vascular imaging using SWNTs.¹¹⁷ These results highlight the clinical potential of SWIR to identify and monitor pathological states such as tumor angiogenesis or cardiovascular lesions, which remain the critical current challenges for many imaging modalities.^{158, 159}

Finally, our studies provided, to the best of our knowledge, the first successful demonstration of multispectral SWIR imaging *in vivo* (see Fig. 11). Using a single, low power excitation source in the NIR, separate SWIR signals could be identified from REs injected into different tumors. Combined with molecular targeting approaches, multispectral

REs have the potential to open a new field of molecular imaging with superior SWIR optical properties.

5. Outlook and Conclusions

The development of next generation optical contrast agents must take into consideration a wide array of physical, chemical and biological design parameters and ultimately be tailored to the specific biomedical application. Contrast agents must be designed to achieve the maximum detection sensitivity in tissue while exhibiting low toxicity and tunable pharmacokinetic behaviors. As our understanding of disease complexity grows, it is also apparent that contrast agents that resolve single molecular attributes may not be able to fully capture the fuller repertoire of molecules necessary to provide readouts for disease states. The next generation probes and imaging system would therefore need to deliver enhanced sensitivity, reliable quantitation, and have the ability to resolve multiple simultaneous signals.

REs are promising candidates for medical imaging due to versatile synthesis and modification chemistries, photostability and relative safety. Furthermore, their bright, tunable luminescence using NIR excitation enables multispectral imaging capabilities with high signal to background values. While long term clearance and toxicity studies in larger animal models are still necessary in order to fully evaluate the clinical applicability of REs, preliminary *in vitro* and *in vivo* mouse studies suggest these materials are significantly safer and more stable than many QD formulations.^{74, 81,124} In addition, the FDA approval of yttrium-90 microspheres for the treatment of patients suffering from liver cancer highlights the possibility for clinical translation of RE materials.¹⁶⁰ Combined with emerging advances in multimodal and SWIR imaging, REs can be used to address a wide variety of biomedical challenges, including deep tissue imaging, real-time drug delivery tracking and multispectral molecular imaging.

Acknowledgments

Support from several funding agencies NIH EB015169, NSF BES 0609000, NSF DGE 0333196 is gratefully acknowledged. We appreciate ongoing collaborations with Professor Charles Roth, Professor Suzie Chen, and Dr. Brian Wall and technical support from our laboratory members, Anthony Kulesa, Jesse Kohl, and Margot Zevon.

References

1. Merlo LMF, Pepper JW, Reid BJ, Maley CC. Cancer as an evolutionary and ecological process. *Nature Reviews Cancer*. 2006; 6:924–935.
2. Sotiriou C, Piccart MJ. Opinion - Taking gene-expression profiling to the clinic: when will molecular signatures become relevant to patient care? *Nature Reviews Cancer*. 2007; 7:545–553.
3. Anderson RR, Ross EV. *Laser-tissue interactions. Cutaneous Laser Surgery*. Mosby: Philadelphia, PA. 1994; 9
4. Graves EE, Weissleder R, Ntziachristos V. Fluorescence molecular imaging of small animal tumor models. *Current Molecular Medicine*. 2004; 4:419–430. [PubMed: 15354872]
5. Welch AJ. The Thermal Response of Laser Irradiated Tissue. *IEEE Journal of Quantum Electronics*. 1984; 20:1471–1481.
6. Matthes R, et al. Revision of guidelines on limits of exposure to laser radiation of wavelengths between 400 nm and 1.4 μ m. *Health Phys*. 2000; 79:431–440. [PubMed: 11007467]

7. Culver J, Akers W, Achilefu S. Multimodality molecular imaging with combined optical and SPECT/PET modalities. *Journal of Nuclear Medicine*. 2008; 49:169–172. [PubMed: 18199608]
8. Willmann JK, van Bruggen N, Dinkelborg LM, Gambhir SS. Molecular imaging in drug development. *Nature Reviews Drug Discovery*. 2008; 7:591–607.
9. Frangioni JV. In vivo near-infrared fluorescence imaging. *Curr Opin Chem Biol*. 2003; 7:626–634. [PubMed: 14580568]
10. Davis ME, Chen Z, Shin DM. Nanoparticle therapeutics: an emerging treatment modality for cancer. *Nature Reviews Drug Discovery*. 2008; 7:771–782.
11. Debbage P, Jaschke W. Molecular imaging with nanoparticles: giant roles for dwarf actors. *Histochemistry and Cell Biology*. 2008; 130:845–875. [PubMed: 18825403]
12. Tan, MC.; Chow, GM.; Ren, L., editors. *Nanostructured Materials For Biomedical Applications*. Transworld Research Network; 2009.
13. Tan, MC.; Chow, GM.; Ren, L.; Zhang, Q. *NanoScience in Biomedicine*. Shi, D., editor. Berlin Heidelberg: Springer; 2009. p. 272-289.
14. Frangioni JV. New technologies for human cancer imaging. *Journal of Clinical Oncology*. 2008; 26:4012–4021. [PubMed: 18711192]
15. Gratton SEA, et al. The effect of particle design on cellular internalization pathways. *Proceedings of the National Academy of Sciences of the United States of America*. 2008; 105:11613–11618. [PubMed: 18697944]
16. Chithrani BD, Ghazani AA, Chan WCW. Determining the size and shape dependence of gold nanoparticle uptake into mammalian cells. *Nano Letters*. 2006; 6:662–668. [PubMed: 16608261]
17. Verma A, Stellacci F. Effect of Surface Properties on Nanoparticle-Cell Interactions. *Small*. 2010; 6:12–21. [PubMed: 19844908]
18. Sperling RA, Parak WJ. Surface modification, functionalization and bioconjugation of colloidal inorganic nanoparticles. *Philosophical Transactions of the Royal Society a-Mathematical Physical and Engineering Sciences*. 2010; 368:1333–1383.
19. Bremer C, Ntziachristos V, Weissleder R. Optical-based molecular imaging: contrast agents and potential medical applications. *European Radiology*. 2003; 13:231–243. [PubMed: 12598985]
20. Hilderbrand SA, Weissleder R. Near-infrared fluorescence: application to in vivo molecular imaging. *Current Opinion in Chemical Biology*. 2010; 14:71–79. [PubMed: 19879798]
21. Weissleder R, Ntziachristos V. Shedding light onto live molecular targets. *Nat Med*. 2003; 9:123–128. [PubMed: 12514725]
22. Azar, FS.; Intes, X. *Translational Multimodality Optical Imaging*. Artech House; 2008.
23. Beuthan J, Minet O, Helfmann J, Herrig M, Muller G. The spatial variation of the refractive index in biological cells. *Physics in Medicine and Biology*. 1996; 41:369–382. [PubMed: 8778819]
24. Backman V, et al. Polarized light scattering spectroscopy for quantitative measurement of epithelial cellular structures in situ. *IEEE Journal of Selected Topics in Quantum Electronics*. 1999; 5:1019–1026.
25. Liu Z, Tabakman S, Welsher K, Dai H. Carbon Nanotubes in Biology and Medicine: In vitro and in vivo Detection, Imaging and Drug Delivery. *Nano research*. 2009; 2:85–120. [PubMed: 20174481]
26. Zhang F, Wang R. NIR Luminescent Nanomaterials for Biomedical Imaging. *Journal of Materials Chemistry B*. 2013
27. Smith AM, Duan H, Mohs AM, Nie S. Bioconjugated quantum dots for in vivo molecular and cellular imaging. *Adv Drug Deliv Rev*. 2008; 60:1226–1240. [PubMed: 18495291]
28. Naczynski DJ, et al. Rare-earth-doped biological composites as in vivo shortwave infrared reporters. *Nature communications*. 2013; 4:2199.
29. Yi GS, Chow GM. Water-soluble NaYF₄: Yb,Er(Tm)/NaYF₄/polymer core/shell/shell nanoparticles with significant enhancement of upconversion fluorescence. *Chemistry of Materials*. 2007; 19:341–343.
30. Reisfeld, R.; Jorgensen, CK. *Lasers and Excited State of Rare Earths* 64–122. New York: Springer-Verlag; 1977.

31. Reisfeld, R.; Jorgensen, CK. Handbook on the Physics and Chemistry of Rare Earth. Gshneidner, JKA.; Eyring, L., editors. New York: Elsevier Scientific Publishers B. V.; 1987. p. 1-99.
32. Carnall WT, Goodman GL, Rajnak K, Rana RS. A systematic analysis of the spectra of the lanthanides doped into single crystal lanthanum fluoride (LaF₃). *J. Chem. Phys.* 1989; 90:3443–3457.
33. Solé, J.; Bausa, L.; Jaque, D. An Introduction to the Optical Spectroscopy of Inorganic Solids. Wiley; 2005.
34. Henderson, B.; Imbusch, GF. Optical Spectroscopy of Inorganic Solids. Oxford University Press, Incorporated; 2006.
35. Moore BF, et al. Lanthanide Clusters with Chalcogen Encapsulated Ln: NIR Emission from Nanoscale NdSe_x. *J. Am. Chem. Soc.* 2011; 133:373–378. [PubMed: 21142152]
36. Kornienko A, et al. Highly NIR-Emissive Lanthanide Polyselenides. *Inorg. Chem.* 2011; 50:9184–9190. [PubMed: 21866912]
37. Tan MC, Naczynski DJ, Moghe PV, Riman RE. Engineering the Design of Brightly-Emitting Luminescent Nanostructured Photonic Composite Systems. *Aust J Chem.* 2013; 66:1008–1020.
38. Kumar GA, Chen CW, Ballato J, Riman RE. Optical characterization of infrared emitting rare-earth-doped fluoride nanocrystals and their transparent nanocomposites. *Chemistry of Materials.* 2007; 19:1523–1528.
39. Wang Q, Tan MC, Zhuo R, Kumar GA, Riman RE. A solvothermal route to size- and phase-controlled highly luminescent NaYF₄:Yb,Er up-conversion nanocrystals. *J. Nanosci. Nanotechnol.* 2010; 10:1685–1692. [PubMed: 20355558]
40. Andelman T, Tan MC, Riman RE. Thermochemical engineering of hydrothermal crystallisation processes. *Mater. Res. Innovations.* 2010; 14:9–15.
41. Tan MC, et al. Synthesis and optical properties of infrared-emitting YF₃:Nd nanoparticles. *J. Appl. Phys.* 2009; 106:063118/063111–063118/063112.
42. Yuan D, Tan MC, Riman RE, Chow GM. Comprehensive Study on the Size Effects of the Optical Properties of NaYF₄:Yb,Er Nanocrystals. *The Journal of Physical Chemistry C.* 2013; 117:13297–13304.
43. Kumar GA, Riman R, Snitzer E, Ballato J. Solution synthesis and spectroscopic characterization of high Er³⁺ content LaF₃ for broadband 1.5 μm amplification. *J. Appl. Phys.* 2004; 95:40–47.
44. Riman RE, Kumar GA, Atakan V, Brennan JG, Ballato J. Engineered solution synthesis of rare-earth nanomaterials and their optical properties. *Proc. SPIE-Int. Soc. Opt. Eng.* 2007; 6707:670707/670701–670707/670711.
45. Mai HX, Zhang YW, Sun LD, Yan CR. Size- and phase-controlled synthesis of monodisperse NaYF₄:Yb,Er nanocrystals from a unique delayed nucleation pathway monitored with upconversion spectroscopy. *Journal of Physical Chemistry C.* 2007; 111:13730–13739.
46. Zhang F, et al. Uniform nanostructured arrays of sodium rare-earth fluorides for highly efficient multicolor upconversion luminescence. *Angewandte Chemie-International Edition.* 2007; 46:7976–7979.
47. Li C, et al. Different Microstructures of β-NaYF₄ Fabricated by Hydrothermal Process: Effects of pH Values and Fluoride Sources. *ChemInform.* 2007; 38 no-no.
48. Fan XP, Pi DB, Wang F, Qiu JR, Wang MQ. Hydrothermal synthesis and luminescence behavior of lanthanide-doped GdF₃ nanoparticles. *Ieee Transactions on Nanotechnology.* 2006; 5:123–128.
49. Yi GS, et al. Synthesis, characterization, and biological application of size-controlled nanocrystalline NaYF₄:Yb,Er infrared-to-visible up-conversion phosphors. *Nano Letters.* 2004; 4:2191–2196.
50. Boyer JC, Vetrone F, Cuccia LA, Capobianco JA. Synthesis of colloidal upconverting NaYF₄ nanocrystals doped with Er³⁺, Yb³⁺ and Tm³⁺, Yb³⁺ via thermal decomposition of lanthanide trifluoroacetate precursors. *Journal of the American Chemical Society.* 2006; 128:7444–7445. [PubMed: 16756290]
51. Yi GS, et al. Synthesis and characterization of high-efficiency nanocrystal up-conversion phosphors: Ytterbium and erbium codoped lanthanum molybdate. *Chemistry of Materials.* 2002; 14:2910–2914.

52. Zeng JH, Su J, Li ZH, Yan RX, Li YD. Synthesis and upconversion luminescence of hexagonal-phase NaYF₄: Yb, Er³⁺, phosphors of controlled size and morphology. *Advanced Materials*. 2005; 17:2119-+.
53. Heer S, Kompe K, Gudel HU, Haase M. Highly efficient multicolour upconversion emission in transparent colloids of lanthanide-doped NaYF₄ nanocrystals. *Advanced Materials*. 2004; 16:2102-+.
54. van de Rijke F, et al. Up-converting phosphor reporters for nucleic acid microarrays. *Nature Biotechnology*. 2001; 19:273-276.
55. Zako T, et al. Development of Near Infrared-Fluorescent Nanophosphors and Applications for Cancer Diagnosis and Therapy. *Journal of Nanomaterials*. 2010
56. Prasad, PN. *Nanophotonics* 129-151. John Wiley & Sons, Inc.; 2004.
57. Nyk M, Kumar R, Ohulchanskyy TY, Bergery EJ, Prasad PN. High Contrast in Vitro and in Vivo Photoluminescence Bioimaging Using Near Infrared to Near Infrared Up-Conversion in Tm³⁺ and Yb³⁺ Doped Fluoride Nanophosphors. *Nano Lett*. 2008; 8:3834-3838. [PubMed: 18928324]
58. Wang F, Liu XG. Recent advances in the chemistry of lanthanide-doped upconversion nanocrystals. *Chemical Society Reviews*. 2009; 38:976-989. [PubMed: 19421576]
59. Chen J, Zhao JX. Upconversion Nanomaterials: Synthesis, Mechanism, and Applications in Sensing. *Sensors*. 2012; 12:2414-2435. [PubMed: 22736958]
60. Auzel F. Upconversion and anti-stokes processes with f and d ions in solids. *Chemical Reviews*. 2004; 104:139-173. [PubMed: 14719973]
61. Ballato O, Riman RE, Snitzer E. Sol-gel synthesis of rare-earth-doped lanthanum halides for highly efficient 1.3- μ m optical amplification. *Optics Letters*. 1997; 22:691-693. [PubMed: 18185630]
62. Singh V, et al. Infrared emissions, visible up-conversion, thermoluminescence and defect centres in Er₃Al₅O₁₂ phosphor obtained by solution combustion reaction. *Applied Physics B-Lasers and Optics*. 2010; 101:631-638.
63. van Saders B, Al-Baroudi L, Tan MC, Riman RE. Rare-earth doped particles with tunable infrared emissions for biomedical imaging. *Optical Materials Express*. 2013; 3:566-573.
64. Tan MC, Kumar GA, Riman RE. Near infrared-emitting Er- and Yb-Er- doped CeF₃ nanoparticles with no visible upconversion. *Opt. Express*. 2009; 17:15904-15910. [PubMed: 19724589]
65. Powell, RC. *Physics of Solid-State Laser Materials*. AIP Press/Springer; 1998.
66. Sudo, S. *Optical Fiber Amplifiers: Materials, Devices, and Applications*. Artech House; 1997.
67. Soga K, et al. NIR Bioimaging: Development of Liposome-Encapsulated, Rare-Earth-Doped Y₂O₃ Nanoparticles as Fluorescent Probes. *European Journal of Inorganic Chemistry*. 2010; 2010:2673-2677.
68. Kamimura M, Kanayama N, Tokuzen K, Soga K, Nagasaki Y. Near-infrared (1550 nm) in vivo bioimaging based on rare-earth doped ceramic nanophosphors modified with PEG-b-poly(4-vinylbenzylphosphonate). *Nanoscale*. 2011; 3:3705-3713. [PubMed: 21792433]
69. Blasse, G.; Grabmaier, BC. *Luminescent materials : with 31 tables*. Berlin: Heidelberg [u.a.]: Springer; 1994.
70. Tan MC, Al-Baroudi L, Riman RE. Surfactant Effects on Efficiency Enhancement of Infrared-to-Visible Upconversion Emissions of NaYF₄:Yb-Er. *ACS Appl. Mater. Interfaces*. 2011; 3:3910-3915. [PubMed: 21870851]
71. Hirano S, Suzuki KT. Exposure, metabolism, and toxicity of rare earths and related compounds. *Environmental Health Perspectives*. 1996; 104:85-95. [PubMed: 8722113]
72. Jalil RA, Zhang Y. Biocompatibility of silica coated NaYF₄ upconversion fluorescent nanocrystals. *Biomaterials*. 2008; 29:4122-4128. [PubMed: 18675453]
73. Zhou JC, et al. Bioimaging and toxicity assessments of near-infrared upconversion luminescent NaYF₄:Yb,Tm nanocrystals. *Biomaterials*. 2011; 32:9059-9067. [PubMed: 21880365]
74. Liu J, Aruguete DM, Murayama M, Hochella MF Jr. Influence of size and aggregation on the reactivity of an environmentally and industrially relevant nanomaterial (PbS). *Environ Sci Technol*. 2009; 43:8178-8183. [PubMed: 19924941]
75. Iyer AK, Khaled G, Fang J, Maeda H. Exploiting the enhanced permeability and retention effect for tumor targeting. *Drug Discovery Today*. 2006; 11:812-818. [PubMed: 16935749]

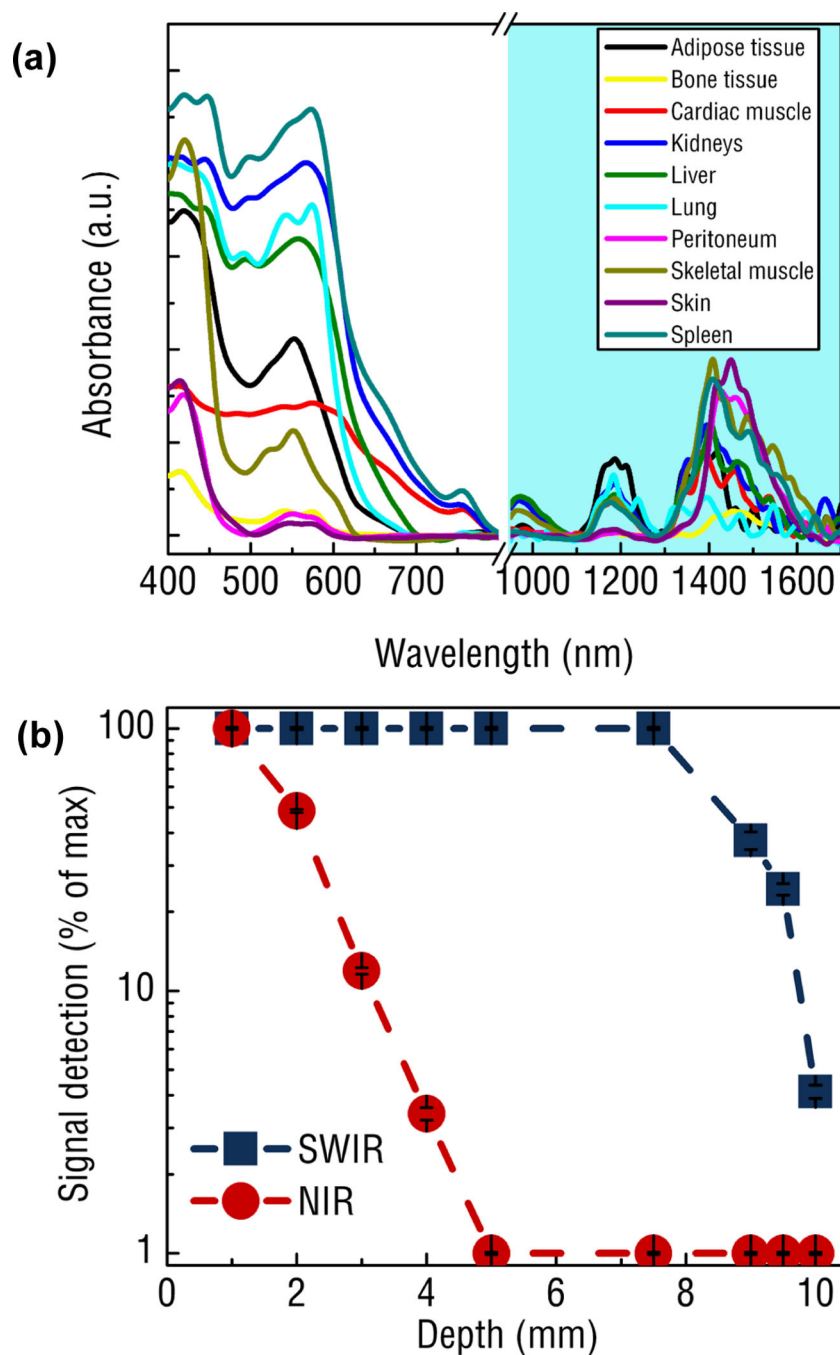
76. Yuan F, et al. Vascular-Permeability in a Human Tumor Xenograft - Molecular-Size Dependence and Cutoff Size. *Cancer Research*. 1995; 55:3752–3756. [PubMed: 7641188]
77. Couvreur P, Vauthier C. Nanotechnology: Intelligent design to treat complex disease. *Pharmaceutical Research*. 2006; 23:1417–1450. [PubMed: 16779701]
78. Hobbs SK, et al. Regulation of transport pathways in tumor vessels: role of tumor type and microenvironment. *Proceedings of the National Academy of Sciences of the United States of America*. 1998; 95:4607–4612. [PubMed: 9539785]
79. Torchilin VP. Recent advances with liposomes as pharmaceutical carriers. *Nature Reviews. Drug Discovery*. 2005; 4:145–160.
80. Tan MC, Ying JY, Chow GM. Interfacial properties and in vitro cytotoxic effects of surface-modified near infrared absorbing Au-Au₂S nanoparticles. *J. Mater. Sci.: Mater. Med.* 2009; 20:2091–2103. [PubMed: 19468832]
81. Ren L, et al. Cisplatin-loaded Au-Au₂S nanoparticles for potential cancer therapy: cytotoxicity, in vitro carcinogenicity, and cellular uptake. *J Biomed Mater Res A*. 2008; 85:787–796. [PubMed: 17896762]
82. Nomura T, Koreeda N, Yamashita F, Takakura Y, Hashida M. Effect of particle size and charge on the disposition of lipid carriers after intratumoral injection into tissue-isolated tumors. *Pharmaceutical Research*. 1998; 15:128–132. [PubMed: 9487559]
83. Hu-Lieskovan S, Heidel JD, Bartlett DW, Davis ME, Triche TJ. Sequence-specific knockdown of EWS-FLI1 by targeted, nonviral delivery of small interfering RNA inhibits tumor growth in a murine model of metastatic Ewing's sarcoma. *Cancer Research*. 2005; 65:8984–8992. [PubMed: 16204072]
84. Boyer JC, Manseau MP, Murray JI, van Veggel FC. Surface modification of upconverting NaYF₄ nanoparticles with PEG-phosphate ligands for NIR (800 nm) biolabeling within the biological window. *Langmuir: the ACS journal of surfaces and colloids*. 2010; 26:1157–1164. [PubMed: 19810725]
85. Idris NM, et al. Tracking transplanted cells in live animal using upconversion fluorescent nanoparticles. *Biomaterials*. 2009; 30:5104–5113. [PubMed: 19539368]
86. Abdul Jalil R, Zhang Y. Biocompatibility of silica coated NaYF(4) upconversion fluorescent nanocrystals. *Biomaterials*. 2008; 29:4122–4128. [PubMed: 18675453]
87. Kumar R, Nyk M, Ohulchanskyy TY, Flask CA, Prasad PN. Combined Optical and MR Bioimaging Using Rare Earth Ion Doped NaYF₄ Nanocrystals. *Advanced Functional Materials*. 2009; 19:853–859.
88. Schafer H, Ptacek P, Kompe K, Haase M. Lanthanide-doped NaYF₄ nanocrystals in aqueous solution displaying strong up-conversion emission. *Chemistry of Materials*. 2007; 19:1396–1400.
89. Li ZQ, Zhang Y. Monodisperse silica-coated polyvinylpyrrolidone/NaYF₄ nanocrystals with multicolor upconversion fluorescence emission. *Angew. Chem. Int. Ed.* 2006; 45:7732–7735.
90. Wang F, et al. Synthesis of polyethylenimine/NaYF₄ nanoparticles with upconversion fluorescence. *Nanotechnology*. 2006; 17:5786–5791.
91. Chatterjee DK, Ruffal AH, Zhang Y. Upconversion fluorescence imaging of cells and small animals using lanthanide doped nanocrystals. *Biomaterials*. 2008; 29:937–943. [PubMed: 18061257]
92. Godbey WT, Wu KK, Mikos AG. Poly(ethylenimine) and its role in gene delivery. *Journal of Controlled Release*. 1999; 60:149–160. [PubMed: 10425321]
93. Moghimi SM, Hunter AC, Murray JC. Long-circulating and target-specific nanoparticles: Theory to practice. *Pharmacological Reviews*. 2001; 53:283–318. [PubMed: 11356986]
94. Choi HS, et al. Design considerations for tumour-targeted nanoparticles. *Nature Nanotechnology*. 2010; 5:42–47.
95. Montet X, Funovics M, Montet-Abou K, Weissleder R, Josephson L. Multivalent effects of RGD peptides obtained by nanoparticle display. *Journal of Medicinal Chemistry*. 2006; 49:6087–6093. [PubMed: 17004722]
96. Davis ME, et al. Evidence of RNAi in humans from systemically administered siRNA via targeted nanoparticles. *Nature*. 2010; 464:U1067–U1140.

97. Xiong L, Yang T, Yang Y, Xu C, Li F. Long-term in vivo biodistribution imaging and toxicity of polyacrylic acid-coated upconversion nanophosphors. *Biomaterials*. 2010; 31:7078–7085. [PubMed: 20619791]
98. Hirano S, Suzuki KT. Exposure, metabolism, and toxicity of rare earths and related compounds. *Environmental health perspectives*. 1996; 104:85. [PubMed: 8722113]
99. Hilderbrand SA, Shao F, Salthouse C, Mahmood U, Weissleder R. Upconverting luminescent nanomaterials: application to in vivo bioimaging. *Chem Commun (Camb)*. 2009:4188–4190. [PubMed: 19585016]
100. Hu H, et al. Multimodal-luminescence core-shell nanocomposites for targeted imaging of tumor cells. *Chemistry*. 2009; 15:3577–3584. [PubMed: 19219877]
101. Abdul Jalil R, Zhang Y. Biocompatibility of silica coated NaYF₄ upconversion fluorescent nanocrystals. *Biomaterials*. 2008; 29:4122–4128. [PubMed: 18675453]
102. Cui S, et al. In vivo targeted deep-tissue photodynamic therapy based on near-infrared light triggered upconversion nanoconstruct. *ACS nano*. 2013; 7:676–688. [PubMed: 23252747]
103. Chen Q, et al. Functionalization of upconverted luminescent NaYF₄: Yb/Er nanocrystals by folic acid–chitosan conjugates for targeted lung cancer cell imaging. *Journal of Materials Chemistry*. 2011; 21:7661–7667.
104. Naczynski DJ, et al. Albumin nanoshell encapsulation of near-infrared-excitable rare-earth nanoparticles enhances biocompatibility and enables targeted cell imaging. *Small*. 2010; 6:1631–1640. [PubMed: 20586056]
105. Cui M, et al. Multifunctional Albumin Nanoparticles As Combination Drug Carriers for Intra-Tumoral Chemotherapy. *Advanced healthcare materials*. 2013
106. Yu M, et al. Laser scanning up-conversion luminescence microscopy for imaging cells labeled with rare-earth nanophosphors. *Anal Chem*. 2009; 81:930–935. [PubMed: 19125565]
107. Ntziachristos V, Bremer C, Weissleder R. Fluorescence imaging with near-infrared light: new technological advances that enable in vivo molecular imaging. *Eur Radiol*. 2003; 13:195–208. [PubMed: 12541130]
108. Frangioni JV. In vivo near-infrared fluorescence imaging. *Curr Opin Chem Biol*. 2003; 7:626–634. [PubMed: 14580568]
109. Prasad, PN. Introduction to Biophotonics 1–10. John Wiley & Sons, Inc.; 2004.
110. Billinton N, Knight AW. Seeing the wood through the trees: A review of techniques for distinguishing green fluorescent protein from endogenous autofluorescence. *Analytical Biochemistry*. 2001; 291:175–197. [PubMed: 11401292]
111. Bashkatov AN, Genina EA, Kochubey VI, Tuchin VV. Optical properties of the subcutaneous adipose tissue in the spectral range 400–2500 nm. *Optics and Spectroscopy*. 2005; 99:836–842.
112. Zonios G, Bykowski J, Kollias N. Skin melanin, hemoglobin, and light scattering properties can be quantitatively assessed in vivo using diffuse reflectance spectroscopy. *Journal of Investigative Dermatology*. 2001; 117:1452–1457. [PubMed: 11886508]
113. Lim YT, et al. Selection of quantum dot wavelengths for biomedical assays and imaging. *Molecular imaging*. 2003; 2:50–64. [PubMed: 12926237]
114. Smith AM, Mancini MC, Nie S. Bioimaging: second window for in vivo imaging. *Nat Nanotechnol*. 2009; 4:710–711. [PubMed: 19898521]
115. Rogach AL, Eychmuller A, Hickey SG, Kershaw SV. Infrared-emitting colloidal nanocrystals: synthesis, assembly, spectroscopy, and applications. *Small*. 2007; 3:536–557. [PubMed: 17340666]
116. Hardman R. A toxicologic review of quantum dots: toxicity depends on physicochemical and environmental factors. *Environ Health Perspect*. 2006; 114:165–172. [PubMed: 16451849]
117. Welsher K, et al. A route to brightly fluorescent carbon nanotubes for near-infrared imaging in mice. *Nat Nanotechnol*. 2009; 4:773–780. [PubMed: 19893526]
118. Dai HJ, et al. High performance in vivo near-IR (>1 μm) imaging and photothermal cancer therapy with carbon nanotubes. *Nano research*. 2010; 3:779–793. [PubMed: 21804931]
119. Schrock E, et al. Multicolor spectral karyotyping of human chromosomes. *Science*. 1996; 273:494–497. [PubMed: 8662537]

120. Medintz IL, Uyeda HT, Goldman ER, Mattoussi H. Quantum dot bioconjugates for imaging, labelling and sensing. *Nature Materials*. 2005; 4:435–446.
121. Tan MC, Connolly J, Riman RE. Optical Efficiency of Short Wave Infrared Emitting Phosphors. *J. Phys. Chem. C*. 2011; 115:17952–17957.
122. Kennedy A, et al. Recommendations for radioembolization of hepatic malignancies using yttrium-90 microsphere brachytherapy: a consensus panel report from the radioembolization brachytherapy oncology consortium. *International journal of radiation oncology, biology, physics*. 2007; 68:13–23.
123. Welsher K, Sherlock SP, Dai H. Deep-tissue anatomical imaging of mice using carbon nanotube fluorophores in the second near-infrared window. *Proc Natl Acad Sci U S A*. 2011; 108:8943–8948. [PubMed: 21576494]
124. Levenson RM, Lynch DT, Kobayashi H, Backer JM, Backer MV. Multiplexing with multispectral imaging: From mice to microscopy. *Ilar Journal*. 2008; 49:78–88. [PubMed: 18172335]
125. Zavaleta CL, et al. Multiplexed imaging of surface enhanced Raman scattering nanotags in living mice using noninvasive Raman spectroscopy. *Proceedings of the National Academy of Sciences of the United States of America*. 2009; 106:13511–13516. [PubMed: 19666578]
126. Zhang Y, Tang Y, Liu X, Zhang L, Lv Y. A highly sensitive upconverting phosphors-based off-on probe for the detection of glutathione. *Sensors and Actuators B: Chemical*. 2013; 185:363–369.
127. Peng J, Wang Y, Wang J, Zhou X, Liu Z. A new biosensor for glucose determination in serum based on up-converting fluorescence resonance energy transfer. *Biosensors & bioelectronics*. 2011; 28:414–420. [PubMed: 21852101]
128. Tu D, et al. Time-resolved FRET biosensor based on amine-functionalized lanthanide-doped NaYF₄:Yb³⁺/Er³⁺@nSiO₂@mSiO₂ Nanospheres as Carriers for Drug Delivery. *The Journal of Physical Chemistry C*. 2011; 115:15801–15811.
129. Wang L, Li Y. Green upconversion nanocrystals for DNA detection. *Chem Commun (Camb)*. 2006:2557–2559. [PubMed: 16779476]
130. Vetrone F, et al. Temperature Sensing Using Fluorescent Nanothermometers. *ACS nano*. 2010; 4:3254–3258. [PubMed: 20441184]
131. Wang C, Cheng L, Liu Z. Drug delivery with upconversion nanoparticles for multi-functional targeted cancer cell imaging and therapy. *Biomaterials*. 2011; 32:1110–1120. [PubMed: 20965564]
132. Kang X, et al. Core-Shell Structured Up-Conversion Luminescent and Mesoporous NaYF₄:Yb³⁺/Er³⁺@nSiO₂@mSiO₂ Nanospheres as Carriers for Drug Delivery. *The Journal of Physical Chemistry C*. 2011; 115:15801–15811.
133. Xu H, et al. Polymer encapsulated upconversion nanoparticle/iron oxide nanocomposites for multimodal imaging and magnetic targeted drug delivery. *Biomaterials*. 2011; 32:9364–9373. [PubMed: 21880364]
134. Cheng L, et al. Highly-sensitive multiplexed in vivo imaging using pegylated upconversion nanoparticles. *Nano research*. 2010; 3:722–732.
135. Xiong L, et al. High Contrast Upconversion Luminescence Targeted Imaging in Vivo Using Peptide-Labeled Nanophosphors. *Anal Chem*. 2009; 81:8687–8694. [PubMed: 19817386]
136. Liu Q, Feng W, Yang T, Yi T, Li F. Upconversion luminescence imaging of cells and small animals. *Nature protocols*. 2013; 8:2033–2044.
137. Liu K, et al. Covalently assembled NIR nanoplatform for simultaneous fluorescence imaging and photodynamic therapy of cancer cells. *ACS nano*. 2012; 6:4054–4062. [PubMed: 22463487]
138. Idris NM, et al. In vivo photodynamic therapy using upconversion nanoparticles as remote-controlled nanotransducers. *Nat Med*. 2012; 18:1580–1585. [PubMed: 22983397]
139. Qian HS, Guo HC, Ho PC, Mahendran R, Zhang Y. Mesoporous-silica-coated up-conversion fluorescent nanoparticles for photodynamic therapy. *Small*. 2009; 5:2285–2290. [PubMed: 19598161]
140. Shan G, Weissleder R, Hilderbrand SA. Upconverting organic dye doped core-shell nanocomposites for dual-modality NIR imaging and photo-thermal therapy. *Theranostics*. 2013; 3:267–274. [PubMed: 23606913]

141. Cheng L, et al. Facile preparation of multifunctional upconversion nanoprobe for multimodal imaging and dual-targeted photothermal therapy. *Angew Chem Int Ed Engl.* 2011; 50:7385–7390. [PubMed: 21714049]
142. Dong B, et al. Multifunctional NaYF₄: Yb³⁺, Er³⁺@Ag core/shell nanocomposites: integration of upconversion imaging and photothermal therapy. *Journal of Materials Chemistry.* 2011; 21:6193–6200.
143. Dai Y, et al. Up-conversion cell imaging and pH-induced thermally controlled drug release from NaYF₄/Yb³⁺/Er³⁺@hydrogel core-shell hybrid microspheres. *ACS nano.* 2012; 6:3327–3338. [PubMed: 22435911]
144. Song C, et al. Characterization and functional analysis of serine proteinase and serine proteinase homologue from the swimming crab *Portunus trituberculatus*. *Fish & shellfish immunology.* 2013
145. Kaijzel EL, van der Pluijm G, Lowik CWGM. Whole-body optical Imaging in animal models to assess cancer development and progression. *Clinical Cancer Research.* 2007; 13:3490–3497. [PubMed: 17575211]
146. Kircher MF, et al. A brain tumor molecular imaging strategy using a new triple-modality MRI-photoacoustic-Raman nanoparticle. *Nature Medicine.* 2012; 18:U829–U235.
147. Kim J, Piao Y, Hyeon T. Multifunctional nanostructured materials for multimodal imaging, and simultaneous imaging and therapy. *Chemical Society Reviews.* 2009; 38:372–390. [PubMed: 19169455]
148. Kircher MF, Mahmood U, King RS, Weissleder R, Josephson L. A multimodal nanoparticle for preoperative magnetic resonance imaging and intraoperative optical brain tumor delineation. *Cancer Research.* 2003; 63:8122–8125. [PubMed: 14678964]
149. Nahrendorf M, et al. Hybrid PET-optical imaging using targeted probes. *Proceedings of the National Academy of Sciences of the United States of America.* 2010; 107:7910–7915. [PubMed: 20385821]
150. Zeng S, Tsang M-K, Chan C-F, Wong K-L, Hao J. PEG modified BaGdF₅:Yb/Er nanoprobe for multi-modal upconversion fluorescent, in vivo X-ray computed tomography and biomagnetic imaging. *Biomaterials.* 2012; 33:9232–9238. [PubMed: 23036962]
151. Pratz G, Carpenter CM, Sun C, Xing L. X-ray luminescence computed tomography via selective excitation: a feasibility study. *IEEE transactions on medical imaging.* 2010; 29:1992–1999. [PubMed: 20615807]
152. Xing H, et al. Multifunctional nanoprobe for upconversion fluorescence, MR and CT trimodal imaging. *Biomaterials.* 2012; 33:1079–1089. [PubMed: 22061493]
153. Liu, J-n, et al. Simultaneous nuclear imaging and intranuclear drug delivery by nuclear-targeted multifunctional upconversion nanoprobe. *Biomaterials.* 33:7282–7290. [PubMed: 22796158]
154. Zhou J, et al. Dual-modality in vivo imaging using rare-earth nanocrystals with near-infrared to near-infrared (NIR-to-NIR) upconversion luminescence and magnetic resonance properties. *Biomaterials.* 2010; 31:3287–3295. [PubMed: 20132982]
155. Lee J, et al. RGD peptide-conjugated multimodal NaGdF₄:Yb³⁺/Er³⁺ nanophosphors for upconversion luminescence, MR, PET imaging of tumor angiogenesis. *Journal of nuclear medicine : official publication, Society of Nuclear Medicine.* 2013; 54:96–103.
156. Zhou J, et al. Fluorine-18-labeled Gd³⁺/Yb³⁺/Er³⁺ co-doped NaYF₄ nanophosphors for multimodality PET/MR/UCL imaging. *Biomaterials.* 2011; 32:1148–1156. [PubMed: 20965563]
157. Wang LV. Multiscale photoacoustic microscopy and computed tomography. *Nature Photonics.* 2009; 3:503–509. [PubMed: 20161535]
158. McDonald DM, Choyke PL. Imaging of angiogenesis: from microscope to clinic. *Nat Med.* 2003; 9:713–725. [PubMed: 12778170]
159. Sanz J, Fayad ZA. Imaging of atherosclerotic cardiovascular disease. *Nature.* 2008; 451:953–957. [PubMed: 18288186]
160. Murthy R, et al. Yttrium-90 microsphere therapy for hepatic malignancy: devices, indications, technical considerations, and potential complications. *Radiographics : a review publication of the Radiological Society of North America, Inc.* 2005; 25(Suppl 1):S41–S55.

161. Desai N. Nanoparticle albumin bound (nab) technology: targeting tumors through the endothelial gp60 receptor and SPARC. *Nanomedicine-Nanotechnology Biology and Medicine*. 2007; 3:339–339.
162. Desai N, Trieu V, Damascelli B, Soon-Shiong P. SPARC Expression Correlates with Tumor Response to Albumin-Bound Paclitaxel in Head and Neck Cancer Patients. *Translational Oncology*. 2009; 2:59–64. [PubMed: 19412420]
163. Podhajcer OL, et al. The role of the extracellular matrix protein SPARC in the dynamic interaction between the tumor and the host. *Cancer and Metastasis Reviews*. 2008; 27:691–705. [PubMed: 18542844]
164. Schnitzer JE, Oh P. Antibodies to Sparc Inhibit Albumin Binding to Sparc, Gp60, and Microvascular Endothelium. *American Journal of Physiology*. 1992; 263:H1872–H1879. [PubMed: 1481911]
165. Vogel SM, Minshall RD, Pilipovic M, Tiruppathi C, Malik AB. Albumin uptake and transcytosis in endothelial cells in vivo induced by albumin-binding protein. *American Journal of Physiology-Lung Cellular and Molecular Physiology*. 2001; 281:L1512–L1522. [PubMed: 11704548]

**Fig. 1.**

Comparing the tissue properties in the SWIR and NIR region for biomedical imaging application: (a) Absorbance spectra of various tissue components spanning from 400 to 1700 nm reveals a distinct region between 900–1300 and 1500–1700 nm exhibiting very low tissue absorbance. Note the break in the spectra from 800 to 900 nm is due to the change from a Si to InGaAs detector in the spectrometer.. (b) Signal intensity of SWIR and NIR light as a function of tissue phantom depth shows complete attenuation of NIR light by 5 mm while SWIR light is able to be detected through 10 mm of phantom tissues.²⁸ Reprinted

(adapted) with permission from Nature Communications. Copyright 2013 © Nature Publishing Group.

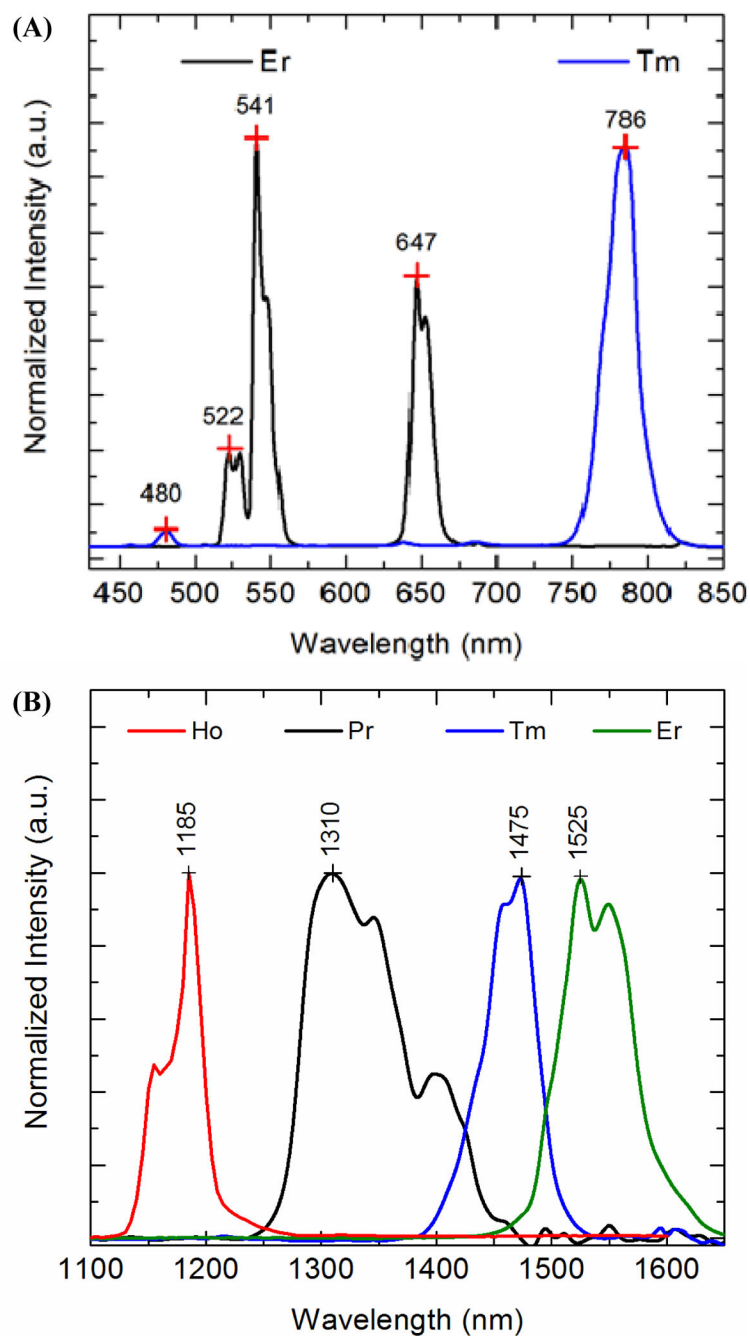


Fig. 2. (a) Visible^{39, 70} and (b) infrared⁶³ emissions from different rare earth doped Yb-sensitized NaYF₄ materials upon excitation at 975 nm.³⁷ Reprinted (adapted) with permission from Australian Journal of Chemistry, Copyright 2013 © CSIRO Publishing Group.

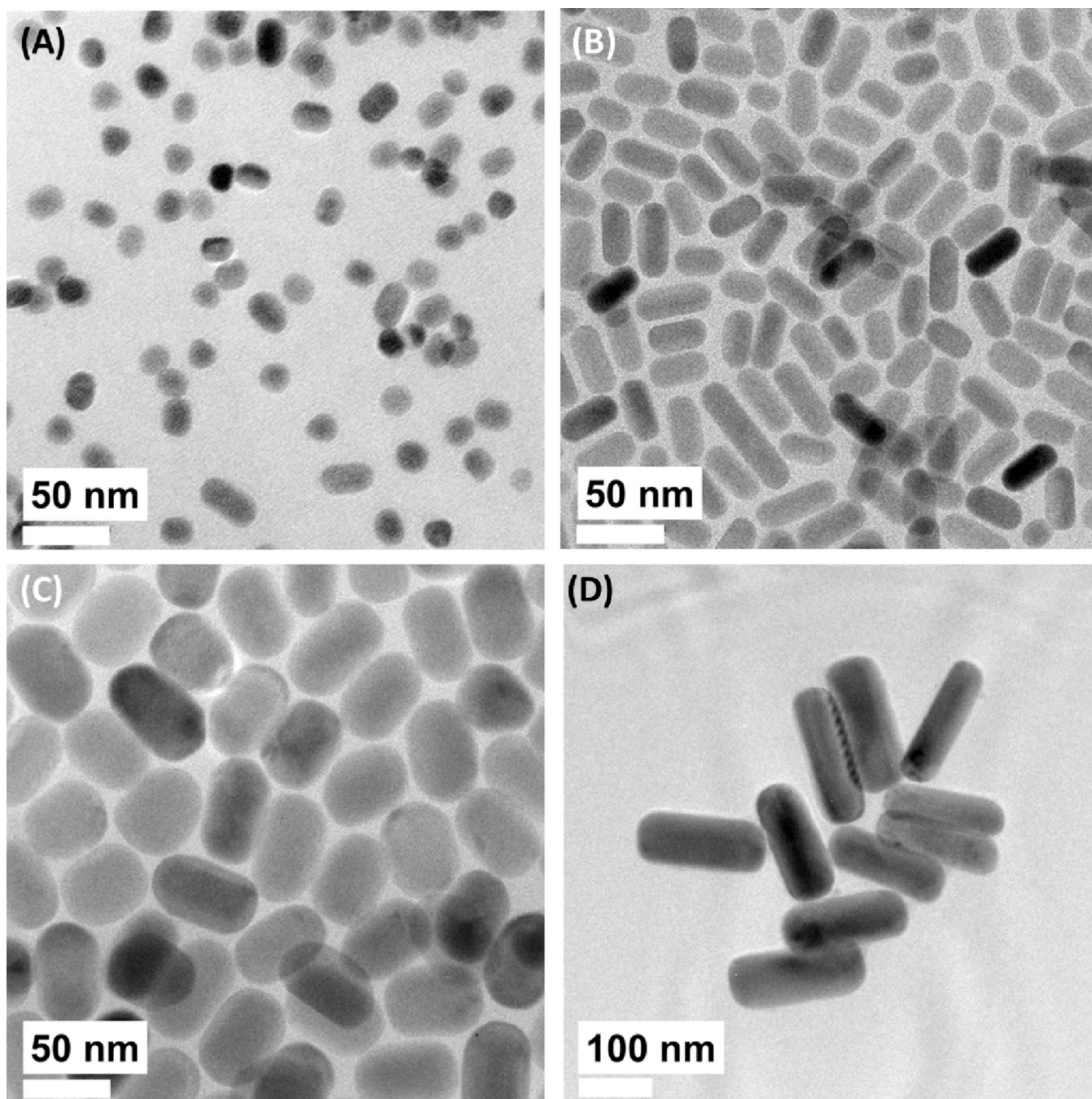


Fig. 3. Solvothermal synthesis of β -NaYF₄:Yb,Er with different sizes and morphologies. (A) 14 nm \times 11 nm, (B) 23 nm \times 16 nm, (C) 53 nm \times 31 nm, and (D) 179 nm \times 63 nm.⁴² Reprinted (adapted) with permission from The Journal of Physical Chemistry C. Copyright 2013 \copyright American Chemical Society.

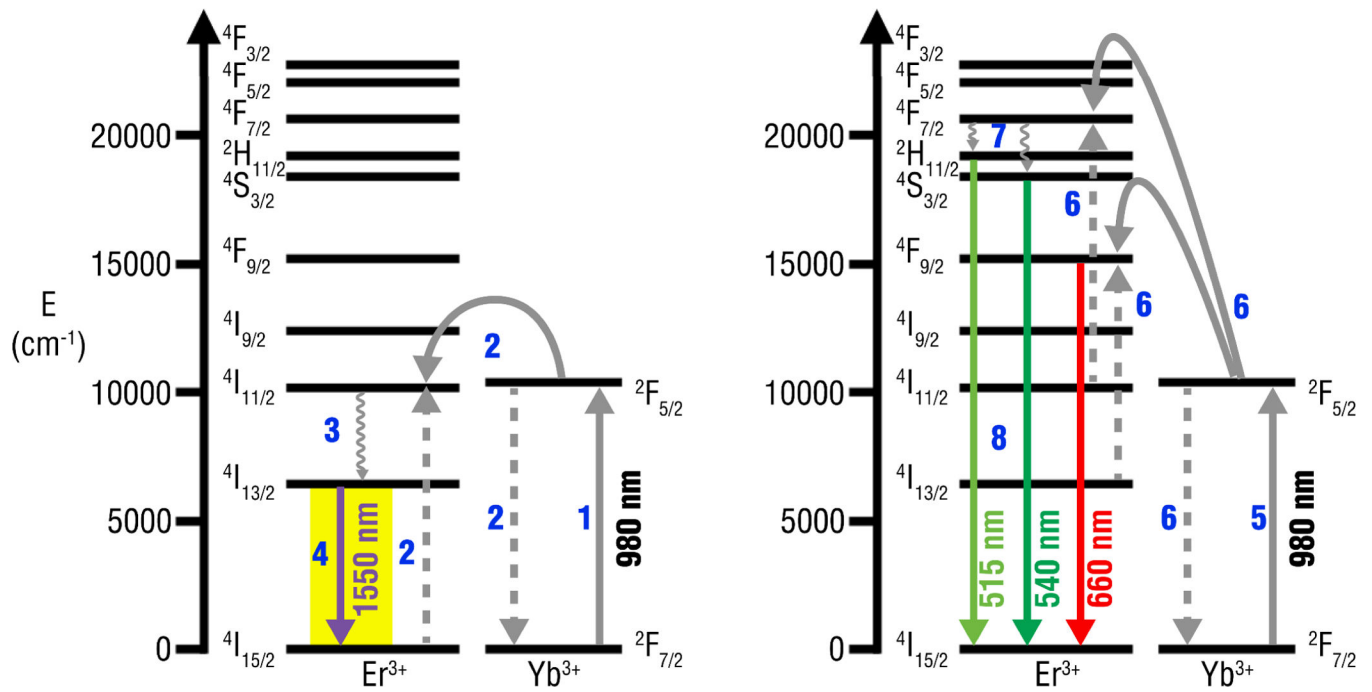


Fig. 4. Typical energy transfer and cross-relaxation pathways of resulting in (a) infrared and (b) visible emissions from Yb, Er doped NaYF_4 materials upon excitation at 980 nm.

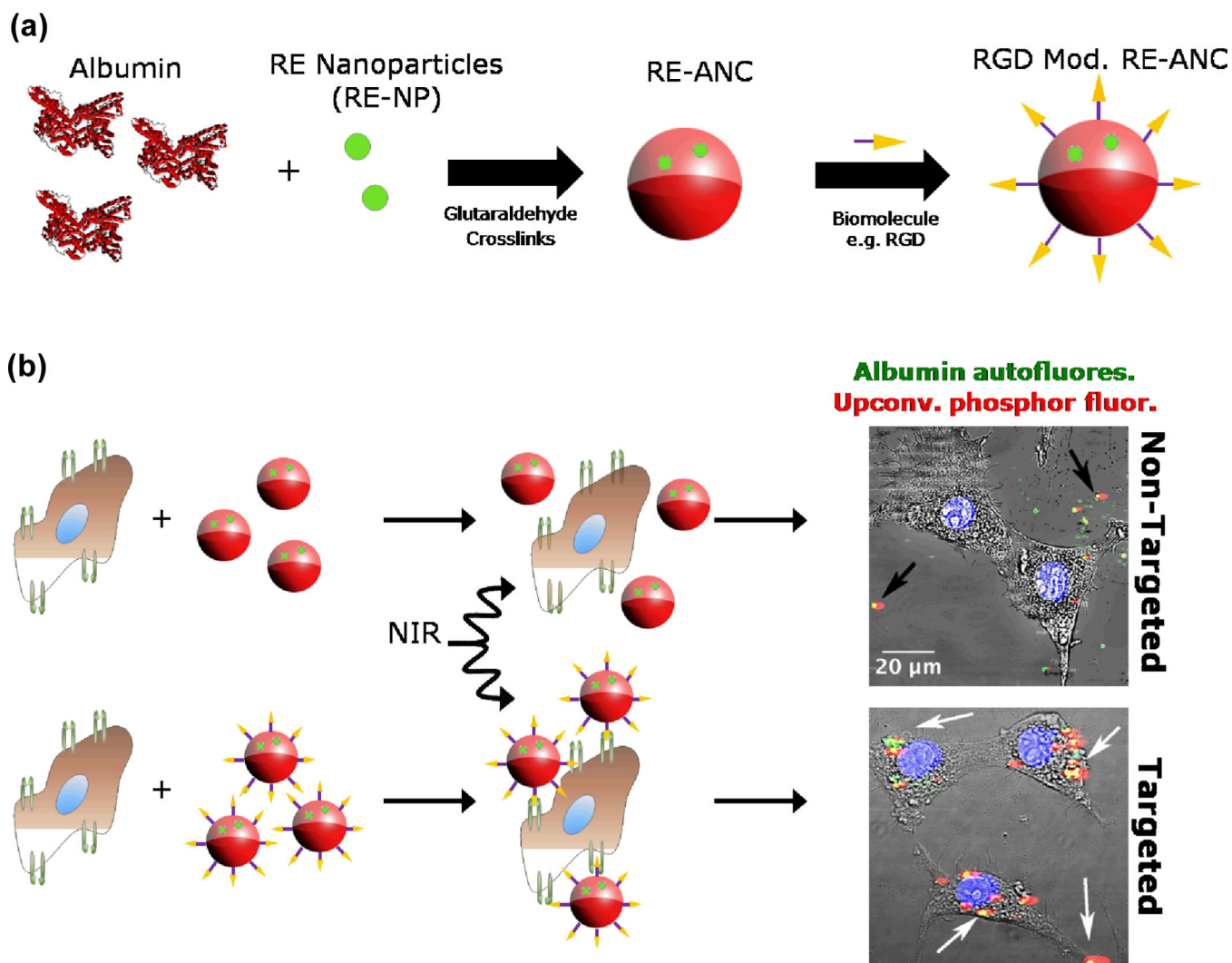


Fig. 5.
(a) Schematic for the cyclic RGD surface modification of albumin-coated REs,¹⁰⁴ and (b) human glioblastoma cells targeted without (top) & with (bottom) cyclic RGD-presenting nanoparticles.³⁷ Reprinted (adapted) with permission from Australian Journal of Chemistry. Copyright 2013 © CSIRO Publishing Group.

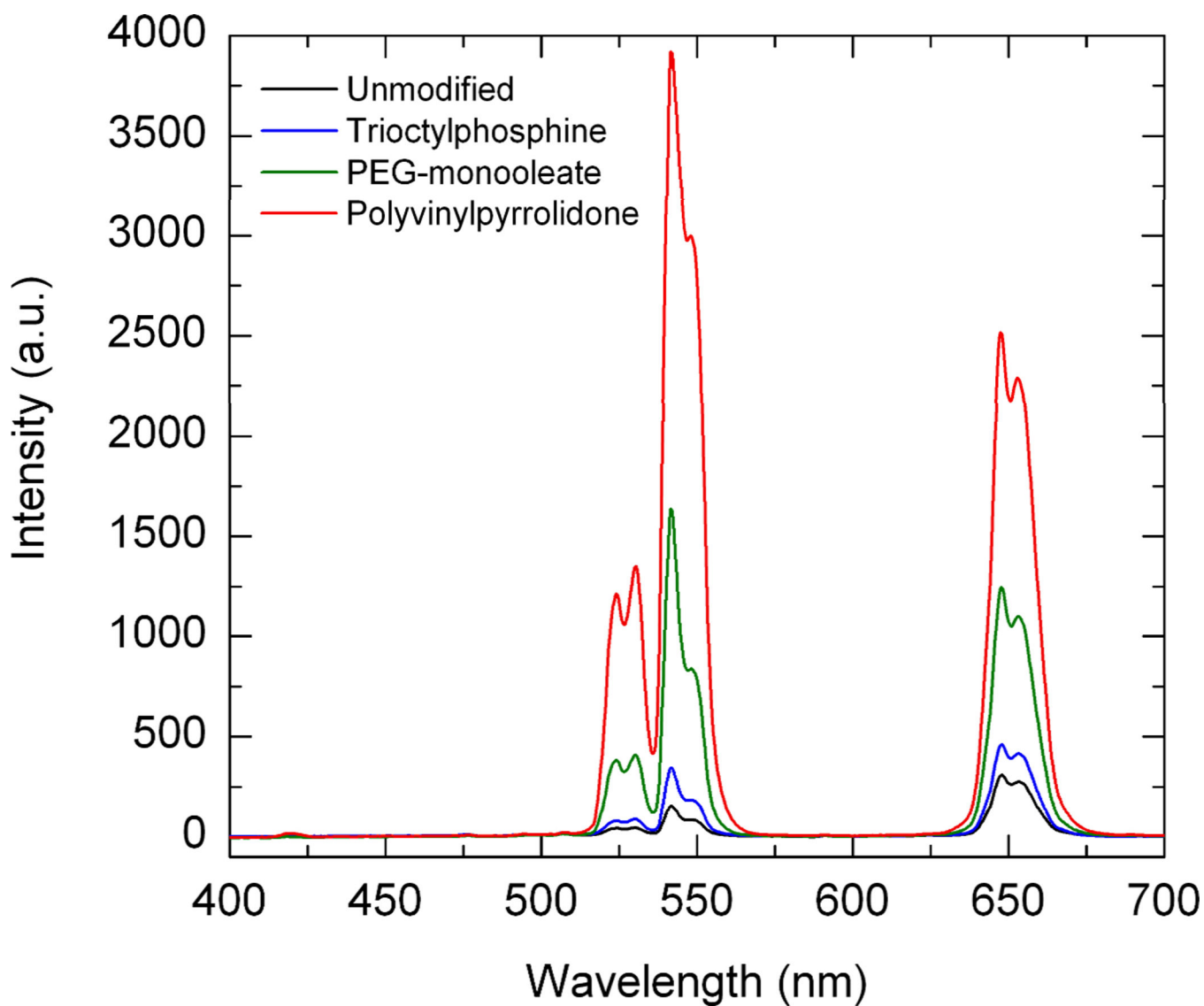
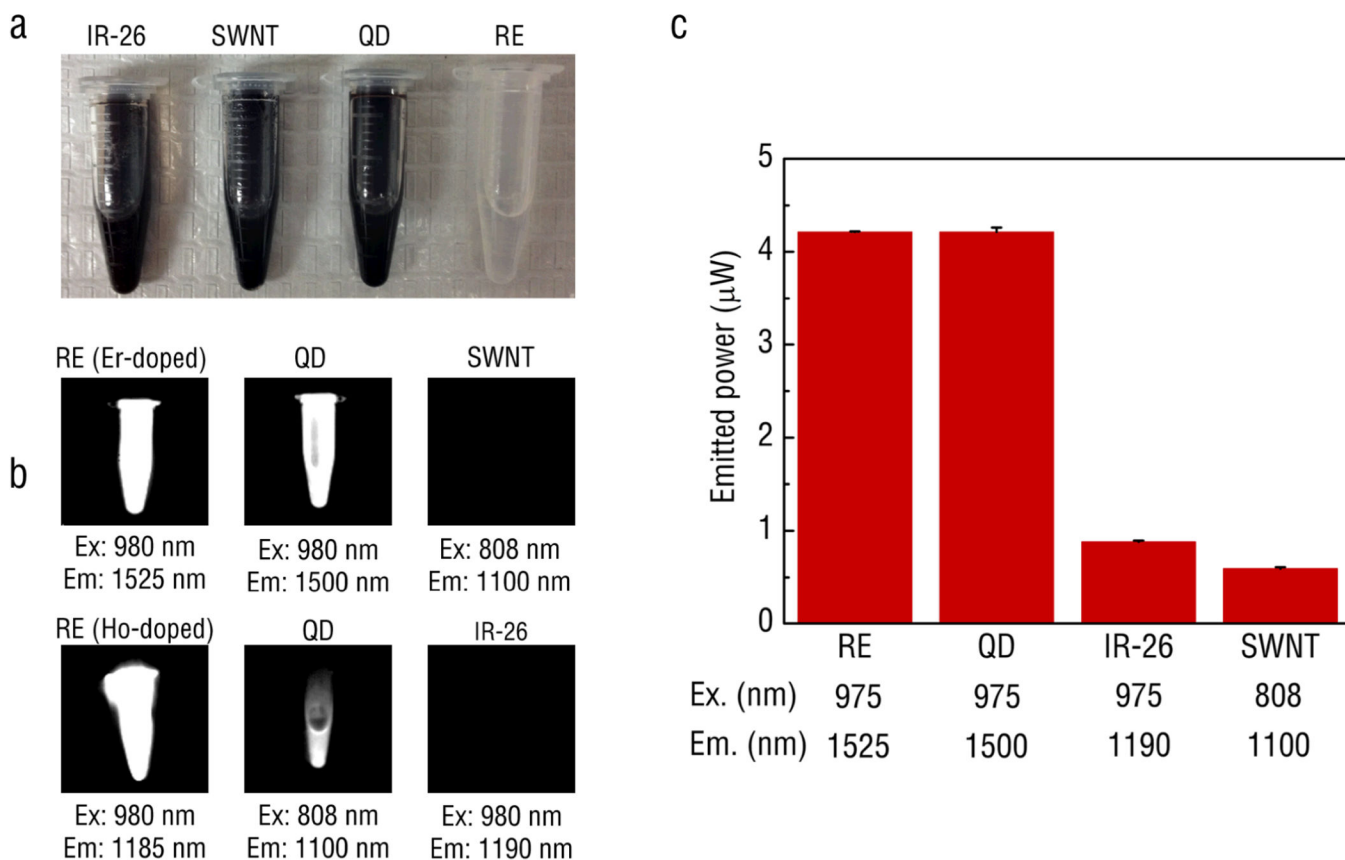


Fig. 6. Surfactant effects on the upconversion emission intensity for the RE's with different adsorbed surfactants.⁷⁰ Reprinted (adapted) with permission from ACS Applied Materials and Interfaces. Copyright 2011 © American Chemical Society.

**Fig. 7.**

A comparison of the performance of various IR-emitting fluorescent probes including IR-26 organic dye, PbS quantum dots, single walled carbon nanotubes and Ho- and Er-doped phosphors: (a) visual image without any excitation and (b) images of IR emissions captured by an InGaAs camera at optimal excitation wavelengths. (c) An integrating sphere was used to quantify the power output of the probes.²⁸ All materials were first dissolved in toluene at 20 mg ml⁻¹ and excited by either 975 nm or 808 nm light at the exact same power (30 μ W). Reprinted (adapted) with permission from Nature Communications. Copyright 2013 © Nature Publishing Group.

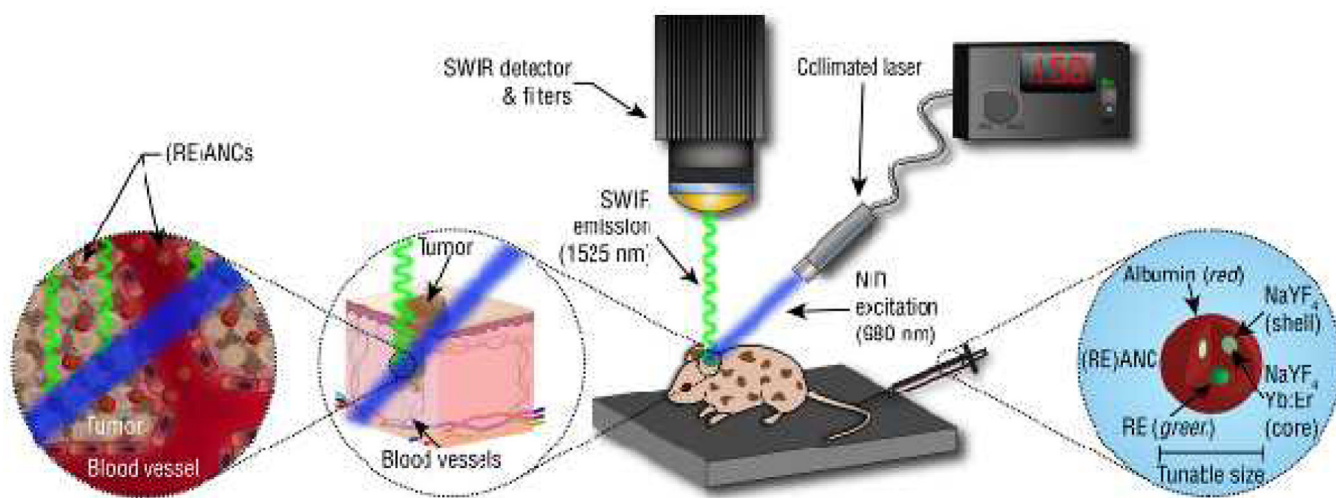


Fig. 8.

Molecular imaging using a customized small animal SWIR imaging platform. Freely circulating albumin-modified REs pass into the tumor interstitial space between the poorly-aligned endothelial cells lining the vasculature. Due to the EPR effect, the albumin modified REs ((RE)ANCs) are retained within the tumors. In addition, the albumin coating may utilize commonly known albumin binding sites and transport pathways to facilitate the passage of the nanoparticles across the tumor endothelium and retention within the tumor microenvironment.^{161–165}

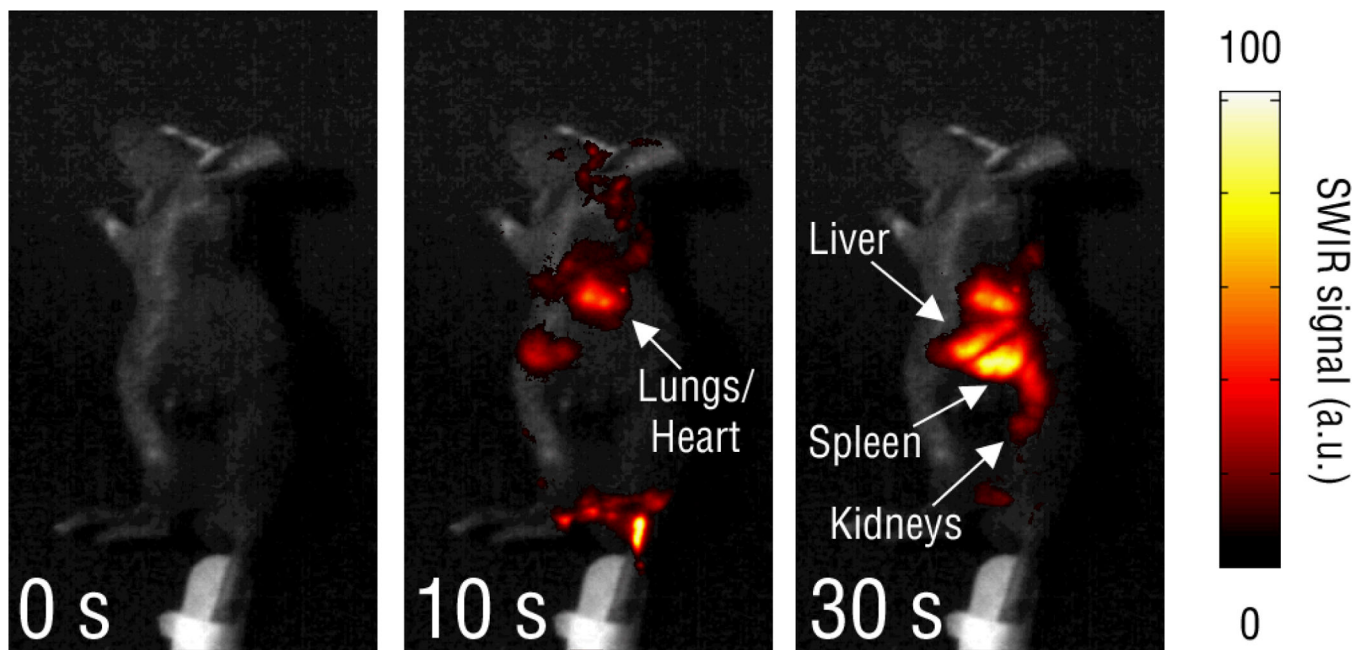


Fig. 9.

Real time imaging of the biodistribution of intravenously injected REs in hairless mice from the left lateral view, where SWIR emission was initially detected in the vasculature of the tail and branching through the abdomen before progressing through the lungs (10 s), liver (30 s) and spleen (30 s). REs were transiently seen in the kidneys (30 s).²⁸ Notably, while lung accumulation is to be avoided in nanoparticle delivery, the signal arising from the lungs was observed shortly after injection and cleared the lungs within minutes. The accumulation of signal in the liver and spleen is consistent with other nanoparticle imaging systems, and was observed to diminish over the course of several days. Reprinted (adapted) with permission from Nature Communications. Copyright 2013 © Nature Publishing Group.

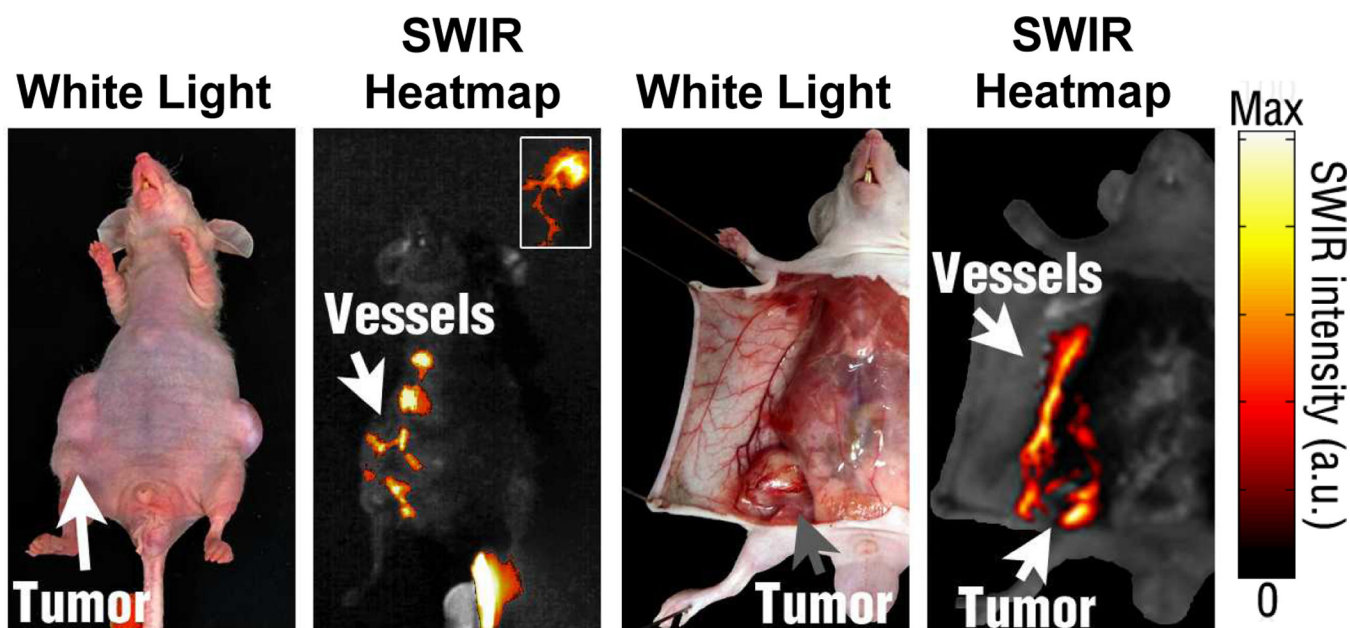


Fig. 10. High-resolution imaging of irregular, branching emission patterns near melanoma xenografts. These patterns were later associated with surrounding vasculature upon dissection of nude mice. Mice were injected with REs intravenously and imaged over time.²⁸ Reprinted (adapted) with permission from Nature Communications. Copyright 2013 © Nature Publishing Group.

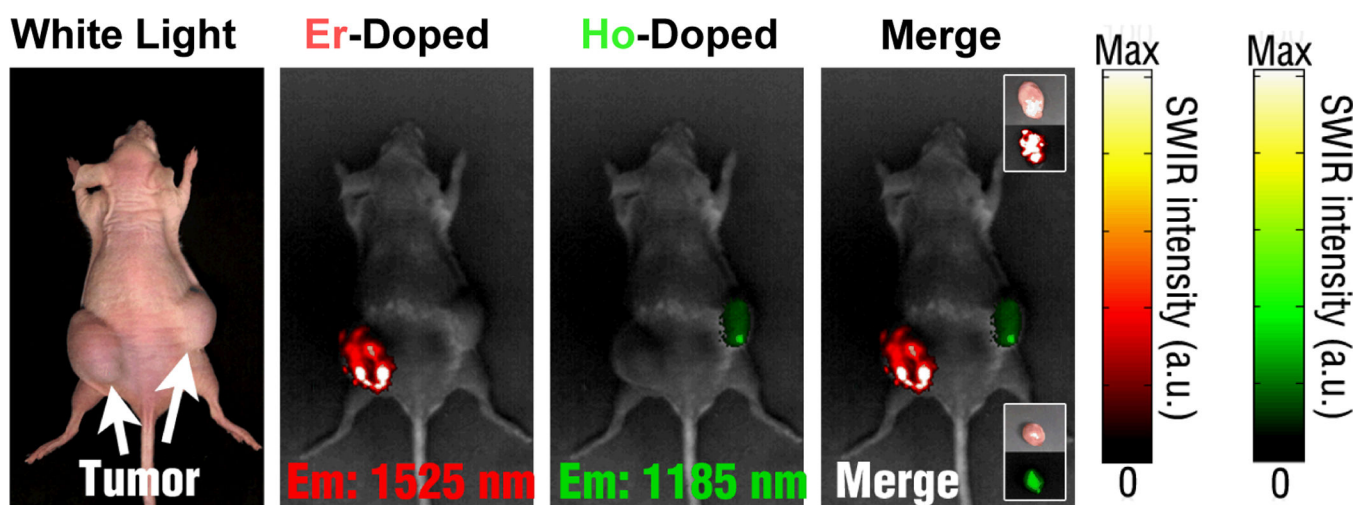


Fig. 11. Multiplexed SWIR imaging for proof of concept was performed with REs doped with Er and Ho emitting at 1525 and 1185 nm, respectively. [in nude mice with developed melanoma xenografts].²⁸ Reprinted (adapted) with permission from Nature Communications. Copyright 2013 © Nature Publishing Group.